PLOS COMPUTATIONAL BIOLOGY

RESEARCH ARTICLE

Mechanistic framework predicts drug-class specific utility of antiretrovirals for HIV prophylaxis

Sulav Duwal[1]*, **Laura Dickinson**[2], **Saye Khoo**[2], **Max von Kleist**[1]*

1 Department of Mathematics & Computer Science, Freie Universität Berlin, Germany, **2** Institute of Translational Medicine, University of Liverpool, United Kingdom

* sulav@zedat.fu-berlin.de (SD); max.kleist@fu-berlin.de (MvK)

Citation: Duwal S, Dickinson L, Khoo S, von Kleist M (2019) Mechanistic framework predicts drug-class specific utility of antiretrovirals for HIV prophylaxis. PLoS Comput Biol 15(1): e1006740. https://doi.org/10.1371/journal.pcbi.1006740

Editor: Sebastian Bonhoeffer, ETH Zürich, SWITZERLAND

Received: December 22, 2017

Accepted: December 20, 2018

Published: January 30, 2019

Data Availability Statement: All relevant data are within the paper and its Supporting Information files.

Funding: MvK. and SD acknowledge financial support from the BMBF e:Bio junior research group 'Systems Pharmacology & Disease Control', grant number 031A307. SK has received funding from Gilead, ViiV Healthcare, Merck and Janssen for the HIV Drug Interactions website, and for research grants. The funders had no role in study design, data collection and analysis, decision to publish, or preparation of the manuscript.

Abstract

Currently, there is no effective vaccine to halt HIV transmission. However, pre-exposure prophylaxis (PrEP) with the drug combination Truvada can substantially decrease HIV transmission in individuals at risk. Despite its benefits, Truvada-based PrEP is expensive and needs to be taken once-daily, which often leads to inadequate adherence and incomplete protection. These deficits may be overcome by next-generation PrEP regimen, including currently investigated long-acting formulations, or patent-expired drugs. However, poor translatability of animal- and *ex vivo*/*in vitro* experiments, and the necessity to conduct long-term (several years) human trials involving considerable sample sizes (N>1000 individuals) are major obstacles to rationalize drug-candidate selection. We developed a prophylaxis modelling tool that mechanistically considers the mode-of-action of all available drugs. We used the tool to screen antivirals for their prophylactic utility and identify lower bound effective concentrations that can guide dose selection in PrEP trials. While *in vitro* measurable drug potency usually guides PrEP trial design, we found that it may over-predict PrEP potency for all drug classes except reverse transcriptase inhibitors. While most drugs displayed graded concentration-prophylaxis profiles, protease inhibitors tended to switch between none- and complete protection. While several treatment-approved drugs could be ruled out as PrEP candidates based on lack-of-prophylactic efficacy, darunavir, efavirenz, nevirapine, etravirine and rilpivirine could more potently prevent infection than existing PrEP regimen (Truvada). Notably, some drugs from this candidate set are patent-expired and currently neglected for PrEP repurposing. A next step is to further trim this candidate set by ruling out compounds with ominous safety profiles, to assess different administration schemes in silico and to test the remaining candidates in human trials.

Author summary

Pre-exposure prophylaxis (PrEP) is a novel, promising strategy to halt HIV transmission. PrEP with Truvada can substantially decrease the risk of infection. However, individuals often inadequately adhere to the once-daily regimen and the drug is expensive. These

Competing interests: The authors have declared that no competing interests exist.

shortcomings may be overcome by next-generation PrEP compounds, including long-acting formulations. However, poor translatability of animal- and *ex vivo*/*in vitro* experiments, and difficulties in conducting long-term trials involving considerable sample sizes ($N > 1000$ individuals) make drug-candidate selection and optimization of administration schemes costly and often infeasible. We developed a simulation tool that mechanistically considers the mode-of-action of all antivirals. We used the tool to screen all available antivirals for their prophylactic utility and identified lower bound effective concentrations for designing PrEP dosing regimen in clinical trials. We found that *in vitro* measured drug potency may over-predict PrEP potency, for all antiviral classes except reverse transcriptase inhibitors. We could rule out a number of antivirals for PrEP repurposing and predicted that darunavir, efavirenz, nevirapine, etravirine and rilpivirine provide complete protection at clinically relevant concentrations. Further trimming of this candidate set by compound-safety and by assessing different implementation schemes is envisaged.

Introduction

Pre-exposure prophylaxis (PrEP) to prevent HIV infection (using drugs which are licensed for its treatment) has been assessed in people at high risk of sexual transmission. Of the available agents, once-daily tenofovir and emtricitabine (Truvada) have been extensively studied, and demonstrate protective efficacy (59–100% [1, 2]) in individuals who are adherent to the medication; conversely poor medication adherence explains the lack of protection observed in some trials [3]. However, major shortcomings of Truvada-based PrEP are its costs [4], a residual infection risk and the necessity for daily drug intake (which often leads to inadequate adherence). These deficits may be overcome by next-generation PrEP regimen, including patent-expired antivirals and long-acting formulations.

Studies assessing next-generation PrEP regimen are underway [5], but rational selection of which agents to advance into PrEP trials based on their intrinsic pharmacology and mode of action has not been comprehensively or systematically undertaken. Moreover, studies have focussed on patent-protected compounds [6], which are likely unaffordable in resource-constrained settings [4] hit hardest by the epidemic.

The considerable sample sizes ($N > 1000$ individuals) and clinical trial duration required (years) to test any new candidate against tenofovir-emtricitabine, and the need to assess regimens with forgiveness for missed dosing or episodic, event-driven PrEP make the current strategy of empirical drug selection costly and prone to failure. We chose to explore an alternative strategy by developing a mathematical modelling tool to assess the per-contact efficacy of anti-HIV drugs. This approach allows prediction of prophylactic utility by integrating drug specific factors (pharmacokinetic/pharmacodynamic (PK/PD) attributes) and attributes of the targeted risk group in order to probe and discard candidates, accelerate drug development and markedly reduce costs. In this work, we are particularly interested in agents where existing patents had already, or are about to expire, in order to maximise the potential impact for low and middle income countries.

Various epidemiological modelling approaches have been used to predict the public health benefits of PrEP [7] and the risk of emergent drug resistance [8–10]. These approaches are highly dependent on *ad hoc* parameter assumptions [11] (specifically the per-contact PrEP efficacy), which may explain the different and contradictory predictions which have emerged.

Knowledge of the per-contact PrEP efficacy, ideally concentration-prophylaxis relationships, are currently lacking and parameters derived from animal models poorly translate into

human efficacy. Concentration-prophylaxis relationships are particularly critical to define lower concentrations in human trials that can attain e.g. $> 90\%$ protection: I.e., ideally a PrEP candidate should be dosed such that the concentrations stay above this target (e.g. 90% protection) and at the same time avoid adverse effects in all individuals. For prophylaxis, there is a general void of information regarding drug-specific and drug-class specific concentration-prophylaxis relationships. While the potency of drugs to inhibit HIV replication can readily be measured *in vitro*, researchers are often unaware that this measure of drug potency may not coincide with the potency to prevent HIV infection (prophylactic potency) and consequently PrEP trial design may be flawed, incurring costs and putting individuals at risk.

In a top-down approach, Hendrix et al. [12] analyzed available clinical data for Truvada to define concentration-prophylaxis relationships. However, this approach is naturally limited to PrEP candidates where sufficient clinical data already exists and is not able to disentangle the potency of the administered drugs from confounding factors. More mechanistic, bottom-up approaches integrate various host- and viral factors [13–18] to predict the probability of viral extinction. Despite their advantages, these approaches conventionally do not establish concentration-prophylaxis relations, or they are specific to particular drugs [17] or drug classes [18].

In this work, we will first analyze the drug-class specific relation between *in vitro* potency and PrEP efficacy and its dependency on the amount- and type of transmitted virus. Utilizing pharmacokinetic and pharmacodynamic data for all treatment-approved drugs, and simulating typical viral exposures during sexual contact, we will then screen all treatment-approved drugs for their PrEP utility and assess the sensitivity of the prophylactic endpoint with regard to uncertainties in viral dynamics parameters and with regard to variabilities in drug concentration, which can typically result from inter-individual metabolic differences or differences in medication adherence. Our central aim is to provide a tool to screen out drug candidates with a lack of- or uncertain prophylactic efficacy.

Methods

Before HIV infection is irreversibly established, viral replication is highly stochastic [19], corroborated by the observation of a low transmission probability per exposure [20, 21] and a low number of founder viruses responsible for establishing infection [22–25]. The stochasticity can be explained by the order in which viral dynamics reactions occur: For example, when a single virus comes into proximity of target cells, it may either be cleared or it may infect the target cell which can eventually lead to systemic infection. In the current work, we will make use of branching process theory [26] to derive analytical solutions for the probability of viral extinction [13, 15], i.e. the probability to hit the absorbing state where all viral compartments go extinct. These solutions can be used directly to benchmark antivirals for their potential to prevent infection as exemplified in the current work, or they can be used to design efficient algorithms for the numerically *exact* simulation of complex prophylactic dosing regimen as proposed in a related article [27].

Prophylactic efficacy

The infection probability $P_{\mathrm{I}}(Y_0)$ for some initial state Y_0 is the complement of the extinction probability $P_{\mathrm{E}}(Y_0)$

$$P_{\mathrm{I}}(Y_0) = 1 - P_{\mathrm{E}}(Y_0), \tag{1}$$

where Y_0 denotes the initial viral population in a replication enabling (target-cell) environment. Throughout the article we will use $Y = [\mathrm{V}, \mathrm{T}_1, \mathrm{T}_2]^T$, i.e. the state of the viral dynamics is defined by infectious viruses, early- and productively infected cells as outlined below. The

extinction probability is defined by

$$P_{\mathrm{E}}(Y_0) \coloneqq \mathbb{P}\left(Y_t = \begin{bmatrix} 0 \\ 0 \\ 0 \end{bmatrix} \middle| \; Y_0 = \begin{bmatrix} \mathrm{V} \\ \mathrm{T}_1 \\ \mathrm{T}_2 \end{bmatrix} \right) \tag{2}$$

for $t \to \infty$. In words, the probability that all viral compartments will eventually go extinct. The prophylactic efficacy φ then denotes the reduction in infection probability *per contact*,

$$\varphi = 1 - \frac{P_{\mathrm{I}}(Y_0|D)}{P_{\mathrm{I}}(Y_0|\varnothing)} \quad (\text{prophylactic efficacy}), \tag{3}$$

where $P_{\mathrm{I}}(Y_0|D)$ and $P_{\mathrm{I}}(Y_0|\varnothing)$ denote the infection probabilities in the presence- and absence of prophylactic drugs D respectively. The term $P_{\mathrm{I}}(Y_0|D)$ was computed using a mathematical model of the viral dynamics (below) and by mechanistically considering the *direct* effects of the distinct antivirals on viral replication whereas $P_{\mathrm{I}}(Y_0|\varnothing)$ is computed analogously, assuming the absence of drug $D = 0$.

Drug-class specific *direct* effects on virus replication

Virus replication dynamics. We adopted the viral dynamics model described in [28, 29]. Although this model is a coarse representation of the molecular events happening during virus replication, it allows to accurately and mechanistically describe the effect of all existing antiretroviral drug classes on viral replication, as demonstrated in e.g. [30], and can be parameterized by available *in vitro* and *clinical* data. Unlike the original model [28, 29] we do not consider macrophages, motivated by the observation that transmitted viruses are not macrophage-tropic [31, 32] and in line with related modelling approaches [13, 14, 33–35]. The model is schematically depicted in Fig 1. The modelled viral replication cycle consists of free infectious viruses, uninfected T-cells, early infected T-cells (T_1) and productively infected T-cells (T_2). Early infected T-cells (T_1) and productively infected T-cells (T_2) denote T-cells prior- and after proviral integration respectively, where the latter produces virus progeny. The term $\mathrm{T}_{\mathrm{u}} = \lambda_{\mathrm{T}}/\delta_{\mathrm{T}}$ denotes the steady state level of uninfected T-cells prior to virus challenge, where λ_{T} denotes the birth and δ_{T} the death rate of uninfected T-cells. During the onset of infection the number viruses are relatively low and the number of uninfected T-cells is fairly unaffected by virus dynamics [33, 36]. Thus, for all computations, we consider the number of uninfected T-cells to be constant, in line with related approaches [14, 15]. The dynamics of the stochastic viral replication model after virus exposure are then defined by six reactions. In absence of antivirals $\varnothing$ we have

$$a_1(\varnothing) = \quad (\mathrm{CL} + \mathrm{CL}_{\mathrm{T}} \cdot \mathrm{T}_{\mathrm{u}}) \cdot V \quad (\text{clearance of free virus; } V \to *) \tag{4}$$

$$a_2(\varnothing) = \quad (\delta_{\mathrm{PIC}} + \delta_{\mathrm{T}_1}) \cdot \mathrm{T}_1 \quad (\text{clearance of early infected cell; } \mathrm{T}_1 \to *) \tag{5}$$

$$a_3(\varnothing) = \quad \delta_{\mathrm{T}_2} \cdot \mathrm{T}_2 \quad (\text{clearance of late infected cell; } \mathrm{T}_2 \to *) \tag{6}$$

$$a_4(\varnothing) = \quad \beta \cdot \mathrm{T}_{\mathrm{u}} \cdot \mathrm{V} \quad (\text{successful infection of a suscept. cell; } V \to \mathrm{T}_1) \tag{7}$$

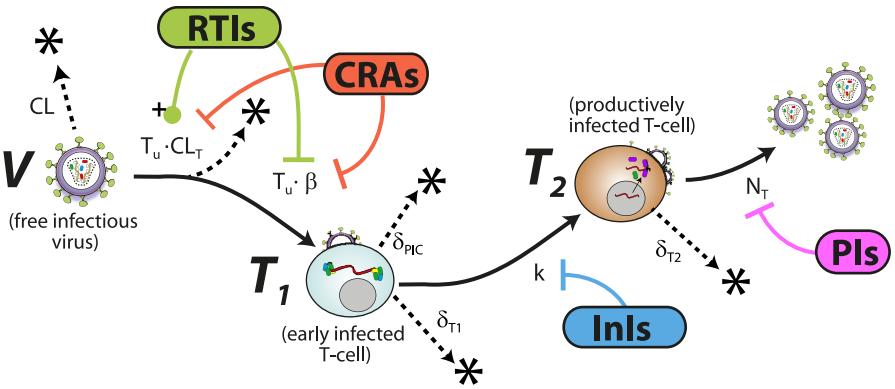

Fig 1. Schematic of the HIV replication cycle and mechanism of interference by treatment-approved drug classes. Free viruses are cleared by the immune system with a rate constant CL. Further, free viruses can be also cleared during unsuccessful T-cell infection CL_T through the destruction of essential viral components of the reverse transcription-, or pre-integration complex [37, 38]. The term β represents the lumped rate of infection of T-cells, including the processes of virus attachment to the cell, fusion and reverse transcription, leading to an early infected cell T_1, before proviral integration. Similarly, the term k denotes the rate by which early infected T_1 cells are transformed into productively infected T_2 cells, involving proviral integration and cellular reprogramming. The term N_T denotes the rate of production of infectious virus progeny by productively infected T_2 cells. The rates β, CL_T, k and N_T may be modified by different antiretrovirals as indicated by bars (inhibition) and pointers with plus sign (drug-dependent increase). The terms $\delta_{T_1} < \delta_{T_2}$ denote the rates of clearance of T_1 and T_2 cells respectively and δ_{PIC} denotes the rate of intracellular destruction of the pre-integration complex. CRA: Co-receptor antagonists, RTIs: reverse transcriptase inhibitors, InIs: Integrase inhibitors, PIs: Protease inhibitors.

https://doi.org/10.1371/journal.pcbi.1006740.g001

$$a_5(\varnothing) = \quad k \cdot T_1 \quad \text{(proviral integration; } T_1 \rightarrow T_2\text{)} \tag{8}$$

$$a_6(\varnothing) = \quad N_T \cdot T_2 \quad \text{(production of infectious virus; } T_2 \rightarrow V + T_2\text{)}, \tag{9}$$

with $CL_T = \left(\frac{1}{\rho_{rev,\varnothing}} - 1\right) \cdot \beta$ in Eq (4) as outlined in [28] where $\rho_{rev,\varnothing} = 0.5$ denotes the probability to successfully complete reverse transcription in the absence of inhibitors [37, 38]. Free viruses are cleared by the immune system with a rate constant CL. Further, free viruses can be also cleared during unsuccessful T-cell infection CL_T through the destruction of essential viral components of the reverse transcription-, or pre-integration complex intracellularly after the virus entered the cell [37, 38]. The term β represents the lumped rate of infection of T-cells, including the processes of virus attachment to the cell, fusion and reverse transcription, leading to an early infected cell T_1, before proviral integration. Similarly, the term k denotes the rate by which early infected T_1 cells are transformed into productively infected T_2 cells, involving proviral integration and cellular reprogramming. The term N_T denotes the rate of production of infectious virus progeny by productively infected T_2 cells (*infectious burst size)*. The terms $\delta_{T_1} < \delta_{T_2}$ denote the rates of clearance of T_1 and T_2 cells respectively and δ_{PIC} denotes the rate of intracellular destruction of the pre-integration complex. Parameters for the viral model are summarized in Table 1 and a mechanistic derivation of the dynamics from first principles is given in [28] (Supplementary Text therein).

Class-specific *direct* drug effects. The *direct* effect of drugs $D \in \{\text{RTI, CRA, InI, PI}\}$ on their target process is typically modelled using the Emax-equation [39]

$$\eta_D(t) = \frac{D_t^m}{IC_{50}^m + D_t^m}, \tag{10}$$

where D_t is the target site concentration of the drug and the term IC_{50} and m denote the drug

concentration at which the targeted process is inhibited by 50% and a hill coefficient [40] respectively. In the current article we will assume that drug concentrations stay constant over the course of infection, which allows to study drug- and drug class specific properties with regard to prophylaxis. This assumption is overcome in related article [27], where pharmacokinetic inputs are explicitly considered to evaluate particular prophylactic dosing regimen.

Reverse transcriptase inhibitors. In the presence of reverse transcriptase inhibitors RTI the reaction propensities a_1 and a_4 are affected [28], i.e.

$$a_1(\mathrm{RTI}) = \left(\mathrm{CL} + \left(\frac{1}{\rho_{rev,\varnothing}} - (1-\eta_{\mathrm{RTI}})\right)\cdot\beta\cdot \mathrm{T_u}\right)\cdot V \tag{11}$$

$$a_4(\mathrm{RTI}) = (1-\eta_{\mathrm{RTI}})\cdot\beta\cdot \mathrm{T_u}\cdot V \tag{12}$$

where $\eta_{\mathrm{RTI}} \in [0, 1]$ follows from Eq (10). Eq (11) results from the specific action of reverse transcriptase inhibitors: they act only after irreversible fusion of viral particles and release of viral contents has occurred by halting reverse transcription, which increases the probability that essential viral constituents get cleared intracellularly preventing viral replication to progress. Thus, inhibition by RTIs can lead to an increase of cell-dependent clearance of viral particles as modelled in Eq (11) (see Supplementary Information of [28] for an explicit derivation). From the equations it becomes evident that the increase in cell-dependent clearance (effect on a_1) matches the reduction in successful infection (effect on a_4). The validity of this model has been assessed in [30].

Other inhibitor classes. Co-receptor antagonists (CRA) decrease the infection propensity a_4 and a_1, whereas integrase inhibitors InI decrease a_5 and protease inhibitors PI reduce a_6 respectively by a factor $(1 - \eta_D)$ [28]:

$$a_1(\mathrm{CRA}) = \left(\mathrm{CL} + (1-\eta_{\mathrm{CRA}})\cdot\left(\frac{1}{\rho_{\mathrm{rev},\varnothing}} - 1\right)\cdot\beta\cdot \mathrm{T_u}\right)\cdot V \tag{13}$$

$$a_4(\mathrm{CRA}) = (1-\eta_{\mathrm{CRA}})\cdot\beta\cdot \mathrm{T_u}\cdot V \tag{14}$$

$$a_5(\mathrm{InI}) = (1-\eta_{\mathrm{InI}})\cdot k\cdot \mathrm{T_1} \tag{15}$$

$$a_6(\mathrm{PI}) = (1-\eta_{\mathrm{PI}})\cdot \mathrm{N_T}\cdot \mathrm{T_2} \tag{16}$$

Note that unlike RTIs, CRAs decrease the adsorption of viral particles by cells, which does not *per se* lead to a cell-dependent clearance of viral particles as in the case of RTIs. InIs block proviral integration, affecting a_5 and PIs prevent maturation, which lowers the amount of *infectious* viruses produced.

Probability of virus extinction

For the ease of notation we introduce the unit vectors $\widehat{\mathrm{V}}$, $\widehat{\mathrm{T}}_1$ and $\widehat{\mathrm{T}}_2$ which represent the states where only one infected compartment is present (either virus, early- or late infected cells)

$$\widehat{\mathrm{V}} = \begin{bmatrix}1\\0\\0\end{bmatrix},\ \widehat{\mathrm{T}}_1 = \begin{bmatrix}0\\1\\0\end{bmatrix},\ \widehat{\mathrm{T}}_2 = \begin{bmatrix}0\\0\\1\end{bmatrix} \tag{17}$$

Table 1. Parameters generally used for the viral dynamics model. Excerpt from [28], except for CL(naive), which assumed that virus clearance is smaller in virus-naive individuals compared to infected individuals, in line with [17, 72]. All parameters refer to the absence of drug treatment ∅. All parameters in units [1/day], except for λ [cells/day] and β [1/day/virus]. Parameter sensitivity was assessed in S2 Text.

Parameter	Value	Reference	Parameter	Value	Reference
λ_T	$2{\cdot}10^9$	[78]	k	0.35	[38]
δ_T, δ_{T_1}	0.02	[79]	β	$8{\cdot}10^{-12}$	[80]
δ_{T_2}	1	[81]	N_T	670	[28, 79]
δ_{PIC}	0.35	[38, 82]	CL(naive)	2.3	[14, 33]

https://doi.org/10.1371/journal.pcbi.1006740.t001

While free virus is typically transmitted, our framework also allows to study prophylactic efficacy for arbitrary initial states. Using the notation above, any state of the system can be expressed as a linear combination of the unit vectors above. For example, $5 \cdot \hat{V} \oplus 3 \cdot \hat{T}_1 \oplus 12 \cdot \hat{T}_2$ denotes the state where we have 5 viruses, 3 early infected cells and 12 late infected cells. In S1 Text we provide a detailed derivation of infection/extinction probabilities after viral exposure. Herein, we will provide a sketch of the central idea.

Starting from a single virus $Y_0 = \hat{V}$, we can write the Chapman-Kolmogorov equation:

$$P_E(Y_0 = \hat{V}) \quad = \quad \sum_{n=0}^{\infty} \mathbb{P}(Y_r = n \cdot \hat{V} | Y_0 = \hat{V}) \cdot P_E(Y_r = \hat{V})^n. \tag{18}$$

In words, the extinction probability $P_E(Y_0 = \hat{V})$ is given by the probability that n viruses are produced in a single replication cycle r, $\mathbb{P}(Y_r = n \cdot \hat{V} | Y_0 = \hat{V})$, and that all of these viruses *eventually* go extinct, considering all possible values of n. Herein we assumed *statistical independence*, i.e. $P_E(Y_r = n \cdot \hat{V}) = P_E(Y_r = \hat{V})^n$. Furthermore, the extinction probabilities for parent- and progeny virus are identical when the inhibitor efficacy is constant, i.e. $P_E(Y_0 = \hat{V}) = P_E(Y_r = \hat{V})$. Next, we construct the embedded Markov chain [26] corresponding from the continuous-time Markov jump model depicted in Fig 1 with parameters in Table 1 (details in S1 Text). This allows to derive algebraic formulas for $\mathbb{P}(Y_r = n \cdot \hat{V} | Y_0 = \hat{V}),\ n = 0 \ldots \infty$. Substituting these into Eq (18), rearranging and solving for $P_E(Y_0 = \hat{V})$ yields a quadratic formula. Solving the quadratic formula, and using $P_E(\cdot) = 1 - P_I(\cdot)$ we derive analytical solutions for the infection probabilities after exposure to a single virus $\hat{V}$, early- $\hat{T}_1$ and late infected cell $\hat{T}_2$:

$$P_I(Y_0 = \hat{V}) = \max\left(0, \frac{a_4(D)}{a_1(D) + a_4(D)} \cdot \frac{a_5(D)}{a_2 + a_5(D)} \left(1 - \frac{1}{R_0(D)}\right)\right) \tag{19}$$

$$P_I(Y_0 = \hat{T}_1) = \max\left(0, \frac{a_5(D)}{a_2 + a_5(D)} \cdot \left(1 - \frac{1}{R_0(D)}\right)\right) \tag{20}$$

$$P_I(Y_0 = \hat{T}_2) = \max\left(0, 1 - \frac{1}{R_0(D)}\right). \tag{21}$$

where $R_0(D)$ denotes the basic reproductive number, i.e. the average number of viruses produced from a single founder virus [41] in a single replication cycle under the action of drug D. Using our model we have $R_0(D) = \frac{a_4(D)}{a_1(D)+a_4(D)} \cdot \frac{a_5(D)}{a_2+a_5(D)} \cdot \frac{a_6(D)}{a_3}$. The first solution $P_I(\cdot) = 0$ of

Eqs (19)–(21) are valid in the regimen where $R_0(D) \leq 1$, i.e. in the regimen where extinction is certain. The second solution describes the case where infection may occur, i.e. $R_0(D) > 1$. The pre-terms in the second solution of Eqs (19) and (20) denote the bottlenecking probabilities that a late-infected, virus producing cell is reached, starting from a free virus (Eq (19)) or starting from an early infected cell (Eq (20)) respectively.

We can assume *statistical independence* during the onset of infection (i.e. competition for target cells is negligible) as noted before. Hence, for any given combination of free virus, early-stage infected cell and late-stage infected cell the extinction probability is given by

$$P_{\mathrm{E}}\left(Y_0 = \begin{bmatrix} \mathrm{V} \\ \mathrm{T}_1 \\ \mathrm{T}_2 \end{bmatrix}\right) = \left(P_{\mathrm{E}}(Y_0 = \widehat{\mathrm{V}})\right)^{\mathrm{V}} \cdot \left(P_{\mathrm{E}}(Y_0 = \widehat{\mathrm{T}}_1)\right)^{\mathrm{T}_1} \cdot \left(P_{\mathrm{E}}(Y_0 = \widehat{\mathrm{T}}_2)\right)^{\mathrm{T}_2}, \quad (22)$$

where the exponents V, T_1 and T_2 denote the number of free virus, early- and late-stage infected cells present and where we notice that $P_{\mathrm{E}}(\cdot) = 1 - P_{\mathrm{I}}(\cdot)$.

Virus exposure model

Initial viral exposure after sexual intercourse occurs at tissue sites typically not receptive for establishing and shedding HIV infection (e.g. mucosal tissues). Hence, the virus needs to pass several bottlenecks and physiological barriers to reach a replication enabling (target-cell) environment where infection can be established and from where it can shed systemically [42]. To determine realistic inoculum sizes after sexual exposure to HIV, we previously developed a data-driven statistical model linking plasma viremia in a transmitter to the initial viral population Y_0 in a replication-enabling environment [18] (Supplementary Note 4 therein for details). Herein, we used the 'exposure model' to compute drug efficacy estimates after homosexual exposure presented in section *Prophylactic efficacy of treatment-approved antivirals*. In brief, this 'exposure model' was developed to capture key clinical observations: (i) the average HIV transmission probabilities per exposure as reported in [20, 21, 43]. (ii) the fact that viral loads in the untreated transmitter population are approximately log-normal distributed [18, 44–46] ($\mu = 4.51$, $\sigma = 0.98$) and (iii) the observation that the plasma viremia in the transmitter is the most dominant factor determining HIV transmission [44, 47–49]. More specifically, it was reported that each 10-fold increase in the transmitter's viral load increases the transmission probability per coitus by approximately 2.45-fold [47] (similar values confirmed in [49]). The aforementioned clinical observations can be summarised in the formula below:

$$\bar{P}_{\mathrm{trans}} = \int_{v=0}^{\infty} P(\mathrm{VL} = v) \cdot \left(\sum_{n=0}^{\infty} P(Y_0 = n \cdot \widehat{\mathrm{V}} | \mathrm{VL} = v) \cdot P_{\mathrm{I}}(Y_0 = n \cdot \widehat{\mathrm{V}})\right) \quad (23)$$

where $\bar{P}_{\mathrm{trans}}$ is the average transmission probability per exposure/coitus (given in (i)), $P(\mathrm{VL} = v)$ is the probability density of viral load in the donor (log-normal distributed, given in (ii)), $P_{\mathrm{I}}(Y_0 = n \cdot \widehat{\mathrm{V}})$ is the infection probability when n viruses reach a replication enabling site (computed from the virus dynamics model above with $P_{\mathrm{I}}(Y_0 = \widehat{\mathrm{V}}) \approx 0.0996$) and $P(Y_0 = n \cdot \widehat{\mathrm{V}} | \mathrm{VL} = v)$ denotes the 'exposure model' (the probability that n viruses reach a replication-enabling compartment after viral exposure from a transmitter with virus load v). For the 'exposure model', we assumed a binomial distribution

$$P(Y_0 = n \cdot \widehat{\mathrm{V}} | \mathrm{VL} = v) = \binom{\lceil v^m \rceil}{n} \cdot r^n \cdot (1 - r)^{\lceil v^m \rceil - n)} \quad (24)$$

where $m = \log_{10}(2.45)$ is given by (iii) [47] and the *success probability r* was estimated in a previous work [18] (Supplementary Note 4 therein), e.g. $r_{\text{homo}} = 3.71 \cdot 10^{-3}$ for homosexual exposure. However, the model can be adapted to the different exposure types (e.g. heterosexual, needle-stick, etc . . .). In this model, the *success probability r* summarises both the extent of local exposure, as well as the probability of passing all bottlenecking physiological barriers and reaching a replication enabling target cell compartment. Lastly, in line with Keele et al. [22], we observed that if infection occurs in our model it is established by a very low number of viruses after homosexual contact and usually by a single founder virus after heterosexual contact.

Results

Relation between direct effects and prophylactic efficacy

Drug-specific inhibition of viral replication can be studied *in vitro*, for example in single-round turnover experiments [40] or even more mechanistically using enzymatic assays in conjunction with appropriate mathematical models [50]. Since the infection risk per exposure is already low in untreated individuals [20, 21], exploring the prophylactic efficacy (reduction in infection risk) in the clinic is difficult, requiring very long (several years) clinical trials with many individuals ($N > 1000$) to achieve statistically evaluable results. Systematic evaluation of concentration-effect relations is not feasible in this context, notwithstanding ethical concerns.

We wanted to gain a deeper insight how *in vitro* measurable direct drug efficacy η translates into prophylactic efficacy φ (reduction in infection probability per exposure) in a drug-class specific manner. Particularly, since different antiviral drug classes inhibit distinct stages in the HIV replication cycle, we wanted to elucidate how these different mechanisms of action affect prophylaxis. We combined Eqs (11)–(16) with Eqs (19)–(21) into Eq (3) to predict prophylactic efficacy. When relating *direct* drug effects η to prophylactic efficacy φ we observed striking drug-class specific differences as illustrated in Fig 2. Using parameters from Table 1 we found that the prophylactic efficacy φ may be less than predicted by *in vitro* measurable direct drug effects η. The sole exception are reverse transcriptase inhibitors (RTI) in case of exposure to a single virus particle $Y_0 = \widehat{V}$ where the two measures of drug efficacy coincide. While the prophylactic efficacy after exposure to a single virus are moderately less than the direct effects of co-receptor antagonists CRA and integrase inhibitors InI respectively (Fig 2A), there is a profound difference for protease inhibitors, which do not seem to reduce HIV transmission unless their direct efficacy η exceeds $\approx 95\%$. Interestingly, a similar observation using a different mathematical model and only distinguishing RTIs and PIs has been made by Conway et al. [13].

While HIV-transmission typically occurs after exposure to free virus, it is still useful to study the prophylactic efficacy of distinct drug classes in the hypothetical case when infected cells were present in the exposed individual. A realistic example for this scenario is post-exposure prophylaxis (PEP): During PEP, drugs are taken shortly *after* virus exposure and initial viral replication steps may have taken place generating early- or late infected cells. As can be seen in Fig 2B and 2C, the prophylactic efficacy of all drugs profoundly deteriorates compared to their direct effects, i.e. only very effective (in terms of η) drugs may prevent systemic infection once cells become infected in the exposed individual. An exception are integrase inhibitors: their prophylactic efficacy φ is moderately less than their direct effect η (panel B) if only early infected cells T_1 (before proviral integration) were present. Thus, while the prophylactic efficacy of all other drug classes is profoundly less than their direct effects once infected cells emerged, integrase inhibitors may still potently prevent infection. An intuitive explanation for the deterioriation of prophylactic efficacy can be made in terms

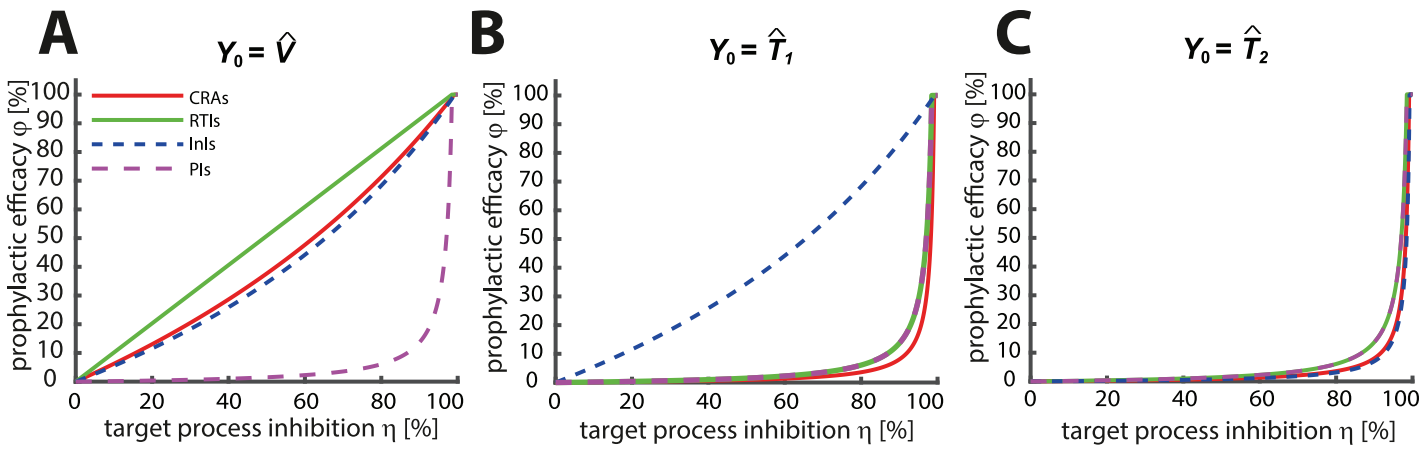

Fig 2. Relation between direct drug effect and prophylactic efficacy. The relation between direct drug effect η and prophylactic efficacy φ (reduction in infection) is shown for different drug classes utilizing the viral model depicted in Fig 1 with parameters stated in Table 1. Panel **A**: Relation between η and φ when a single virus $Y_0 = \hat{V}$ reached a replication-enabling compartment in the virus-exposed individual. Panel **B**: Relation between η and φ when a single early infected cell $Y_0 = \hat{T}_1$ or (panel **C**) a late infected T-cell $Y_0 = \hat{T}_2$ reached a replication-enabling compartment. Solid red lines: CRAs, solid green line: RTIs, dashed blue line: InI, dashed purple line: PIs.

https://doi.org/10.1371/journal.pcbi.1006740.g002

of changes in drug-target stoichiometry: For example, after exposure to a single virus $\hat{V}$, drugs from the classes of CRAs, RTIs and InIs need to block a single reaction to foster viral extinction. For PIs however, the same is only achieved if maturation of the entire viral progeny is inhibited (possibly hundreds of particles). Similarly, when considering a single early infected cell $\hat{T}_1$, CRAs and RTIs can only prevent further viral expansion *after* viral progeny has emerged. Subsequently, for each viral particle (possibly hundreds) the respective target processes (receptor binding, reverse transcription) need to be blocked by the inhibitors. Along the same lines of argumentation it is also evident that prophylactic efficacy is generally more favourable in the case of PrEP, compared to post-exposure prophylaxis (PEP), where initial viral replication may have occurred.

In vitro drug potency may overestimate PrEP potency

In vitro measured drug potency IC_{50}, IC_{90} usually guides the design of PrEP trials [51]. In particular, dosing regimen are designed so that the majority of individuals achieve drug levels just above the 90% inhibitory concentrations IC_{90}. However, it has never been rigorously investigated whether these 'target concentrations' are sufficient to provide 90% protection against HIV infection. Integrating Eq (10) into Eqs (11)–(16), (19) and (3) allows to predict the concentration-prophylaxis profile for different HIV-1 inhibitor classes. Rearranging this composite equation reveals how *in vitro* measured drug potency IC_{50}, IC_{90} can be translated into prophylactic potency (50% and 90% reduction in infection risk, EC_{50} and EC_{90}, respectively), guiding clinical trial design. The derived analytical expressions for the prophylactic efficacy (reduction in infection risk) indicate that the shape of the concentration-prophylaxis profile varies considerably for different HIV-1 inhibitor classes with important consequences for their prophylactic endpoints (% reduction in HIV transmissibility).

After exposure to a single virion $Y_0 = \hat{V}$, the overall shape of the concentration-prophylaxis profile for co-receptor antagonists (CRAs), reverse transcriptase inhibitors (RTIs) and integrase inhibitors (InIs) is a classical Emax equation (the equation of choice for evaluating

concentration-effect relations), see S1 Text for derivation.

$$\varphi(\widehat{\mathrm{V}}) = \tfrac{R_0(\varnothing)}{R_0(\varnothing)-1} \cdot \frac{D^m}{\mathrm{IC}_{50}^m\left(\frac{1}{\upsilon}\right) + D^m} \overset{R_0(\varnothing)\gg 1}{\approx} \frac{D^m}{\mathrm{EC}_{50}^m + D^m} \qquad \text{(CRA)} \tag{25}$$

$$\varphi(\widehat{\mathrm{V}}) = \tfrac{R_0(\varnothing)}{R_0(\varnothing)-1} \cdot \frac{D^m}{\mathrm{IC}_{50}^m + D^m} \overset{R_0(\varnothing)\gg 1}{\approx} \frac{D^m}{\mathrm{EC}_{50}^m + D^m} \qquad \text{(RTI)} \tag{26}$$

$$\varphi(\widehat{\mathrm{V}}) = \tfrac{R_0(\varnothing)}{R_0(\varnothing)-1} \cdot \frac{D^m}{\mathrm{IC}_{50}^m\left(\frac{1}{\vartheta}\right) + D^m} \overset{R_0(\varnothing)\gg 1}{\approx} \frac{D^m}{\mathrm{EC}_{50}^m + D^m} \qquad \text{(InI)} \tag{27}$$

where D denotes the concentration of the drug in the blood plasma, m is a slope parameter and IC_{50} denotes the plasma concentration of the drug that inhibits the targeted process (co-receptor binding, reverse transcription or proviral integration) by 50 percent. This parameter can typically be measured *in vitro*, e.g. using single-round turnover experiments [40] and is stated in Table 2 for various drugs. Parameters $\upsilon = \frac{\mathrm{CL}\cdot\rho_{\mathrm{rev},\varnothing}}{\mathrm{CL}\cdot\rho_{\mathrm{rev},\varnothing}+\beta\cdot \mathrm{T_u}} < 1$ and $\vartheta = \frac{\delta_{\mathrm{PIC}}+\delta_{\mathrm{T_1}}}{\delta_{\mathrm{PIC}}+\delta_{\mathrm{T_1}}+k} < 1$ denote the respective probabilities, in the absence of drugs, that the virus is eliminated before entering a host cell, and that essential virus compartments get cleared intracellularly after reverse transcription and before provirus integration. The parameter EC_{50} denotes the plasma concentration of the drug that decreases the probability of infection by 50%, i.e. the *prophylactic potency* of the drug. $R_0(\varnothing)$ denotes the basic reproductive number in the absence of drugs, i.e. the average number of viruses produced from a single founder virus [41] in a single replication cycle when no antivirals were present ($R_0(\varnothing) \approx 67$ according to the utilized model). When the target cell density is sufficiently high (herein considered as a target cell environment), we have $R_0(\varnothing) \gg 1$ and hence the left-side scaling factor in Eqs (25)–(27) will be close to one, $R_0(\varnothing)/(R_0(\varnothing) - 1) \approx 1$. An analysis with low target cell densities is provided in S2 Text.

In case of exposure to a single virus particle $\widehat{\mathrm{V}}$, the slope parameters in the right-most equations coincide with the slope parameter for the respective drug-targeted process m (Eq (10)), stated in Table 2. Notably, for RTIs, we have $\mathrm{EC}_{50} \approx \mathrm{IC}_{50}$, i.e. the drugs potency measured *in vitro* in single-round turnover experiments [40] directly translates into its potency to prevent infection. Using parameters from Table 1 we observe $\mathrm{EC}_{50} > \mathrm{IC}_{50}$ for CRAs and InIs, i.e. compared to their *in vitro* potency, they are less potent in preventing infection. This is largely due to the respective factors ϑ^{-1}, $\upsilon^{-1} > 1$, compare Fig 3A–3C. For InIs this observation is robust across a broad range of parameter values, as shown in S2 Text. Consequently, for InIs, higher concentrations are required to prevent infection than suggested after conducting the respective *in vitro* experiments. For CRAs, predictions are parameter dependent, S2 Text. Rearranging Eqs (25)–(27) allows to directly compute the drug concentration that prevents infection with x percent probability (the EC_x) from the corresponding *in vitro* 50% inhibitory concentration IC_{50} (derivations in S3 Text): In case of exposure *to a single virus particle* we get

$$\mathrm{EC}_x = \mathrm{IC}_{50} \cdot \left(F \cdot \frac{x}{100 \cdot C - x}\right)^{1/m}, \tag{28}$$

where EC_x is the drug concentration that achieves x percent of prophylactic efficacy and the

Table 2. Pharmacodynamic and pharmacokinetic parameters. IC_{50} [nM] and m [unit less] values are available from single turnover experiments in primary peripheral blood mononuclear cells supplemented with 50% human serum from Shen et al. [40], Laskey et al. [92] (DTG) and Jilek at al. [93] (MVC). Because some compounds are highly protein bound, IC_{50} values had to be adjusted for protein binding as outlined in the S5 Text. Indicated values are after protein adjustment. IC_{50} values are reported to be log normal distributed and m values to be normal distributed [40, 93] with respective coefficients of variation $CV = 100 \cdot \sigma/\mu$ [%]. Parameters C_{min} and C_{max} refer to the minimum and maximum concentrations in [nM] during chronic administration using the standard dosing regimen, taken from Shen et al. [40] except those for DTG [94], RPV [95] and MVC [96] (150mg twice daily). $t_{1/2}$—half life of the drug in [hr], f_b—fraction of the drug bound to plasma proteins in [%]. [+]These values were fixed to the typical parameter distributions observed for all other compounds. [◇]Parameters were taken from Drug Bank when available https://www.drugbank.ca/, accession numbers: DB04835, DB00625, DB00238, DB00705, DB08864, DB06817, DB09101, DB08930, DB01072, DB00701, DB01264, DB00224, DB00220, DB00932 or [♭]PubChem https://pubchem.ncbi.nlm.nih.gov, id: 92727. When parameters were not readily available in these databases, parameters were obtained from the indicated literature source. MVC -maraviroc, EFV -efavirenz, NVP -nevirapine, DLV -delavirine, ETR -etravirine, RPV -rilpivirine, RAL -raltegravir, EVG -elvitegravir, DTG -dolutegravir, ATV -atazanavir, APV -amprenavir, DRV -darunavir, IDV -indinavir, LPV -lopinavir, NFV -nelfinavir, SQV -saquinavir, TPV -tipranavir.

Class	Name	IC_{50}	(CV)	m	(CV)	C_{min}	C_{max}	f_b	$t_{1/2}$
CRA	MVC	5.06	(290)	0.61	(27.9)	45	557	76◇	14◇
RTI	EFV	10.7	(16.7)	1.69	(4.73)	5630	12968	99.4 [83]	40◇
RTI	NVP	116	(31.2)	1.55	(9.68)	10883	25153	60◇	45◇
RTI	DLV	336	(44.7)	1.56	(11.5)	10672	27134	98 [84]	5.8◇
RTI	ETR	8.59	(16.3)	1.81	(12.7)	688	1617	99.9 [85]	35 [86]
RTI	RPV	7.73	(17.9)	1.92	(10.4)	177	470	99.1◇	44.5◇
InI	RAL	25.5	(12.1)	1.1	(4.55)	203	3996	83◇	9◇
InI	EVG	55.6	(43.8)	0.95	(4.21)	301	1661	99◇	8.7◇
InI	DTG	89.0	(25.3+)	1.3	(15.4+)	2918	8471	98.9◇	14.5 [87]
PI	ATV	23.9	(11.8)	2.69	(10.4)	899	6264	86 [88]	7◇
PI	APV	262	(12.6)	2.09	(6.70)	2870	14319	90◇	7.1◇
PI	DRV	45.0	(21.6)	3.61	(8.86)	5081	14783	95 [85]	15◇
PI	IDV	130	(11.0)	4.53	(7.94)	1827	12508	60 [89]	1.8◇
PI	LPV	70.9	(20.1)	2.05	(5.85)	8757	15602	99 [60]	2.5♭
PI	NFV	327	(26.8)	1.81	(12.7)	2285	5104	98◇	3.5◇
PI	SQV	88.0	(9.7)	3.68	(6.25)	897	13282	97 [90]	3.9 [91]
PI	TPV	483	(18.0)	2.51	(14.3)	35598	77585	99.9◇	5◇

https://doi.org/10.1371/journal.pcbi.1006740.t002

term $F \geq 1$ is a drug class specific factor

$$F = \begin{cases} \left(\mathrm{CL} + \frac{\beta \cdot \mathrm{T_u}}{\rho}\right)/\mathrm{CL}, & \text{for CRA} \\ 1, & \text{for RTI} \\ 1/\vartheta, & \text{for InI.} \end{cases} \tag{29}$$

and

$$C \coloneqq \frac{R_0(\varnothing)}{R_0(\varnothing) - 1} \approx 1, \tag{30}$$

if $R_0(\varnothing) \gg 1$. Importantly, when exposure to multiple viruses occurs, the concentration-prophylaxis profile is no longer an Emax equation for any inhibitor class, Fig 3A–3C. Furthermore, the slope parameter increases and the EC_{50} may exceed the *in vitro* measurable IC_{50} value. At large inoculum, the corresponding profiles become switch-like. For protease inhibitors (PIs), we derive a power function to describe their prophylactic efficacy (mechanistic derivation in S1 Text):

$$\varphi(\widehat{\mathrm{V}}) = \frac{1}{R_0(\varnothing) - 1} \cdot \frac{D^m}{\mathrm{IC}_{50}^m} = C \cdot \frac{D^m}{\mathrm{IC}_{50}^m} \quad \text{(PI)} \qquad \text{for } 0 \leq \varphi \leq 1, \tag{31}$$

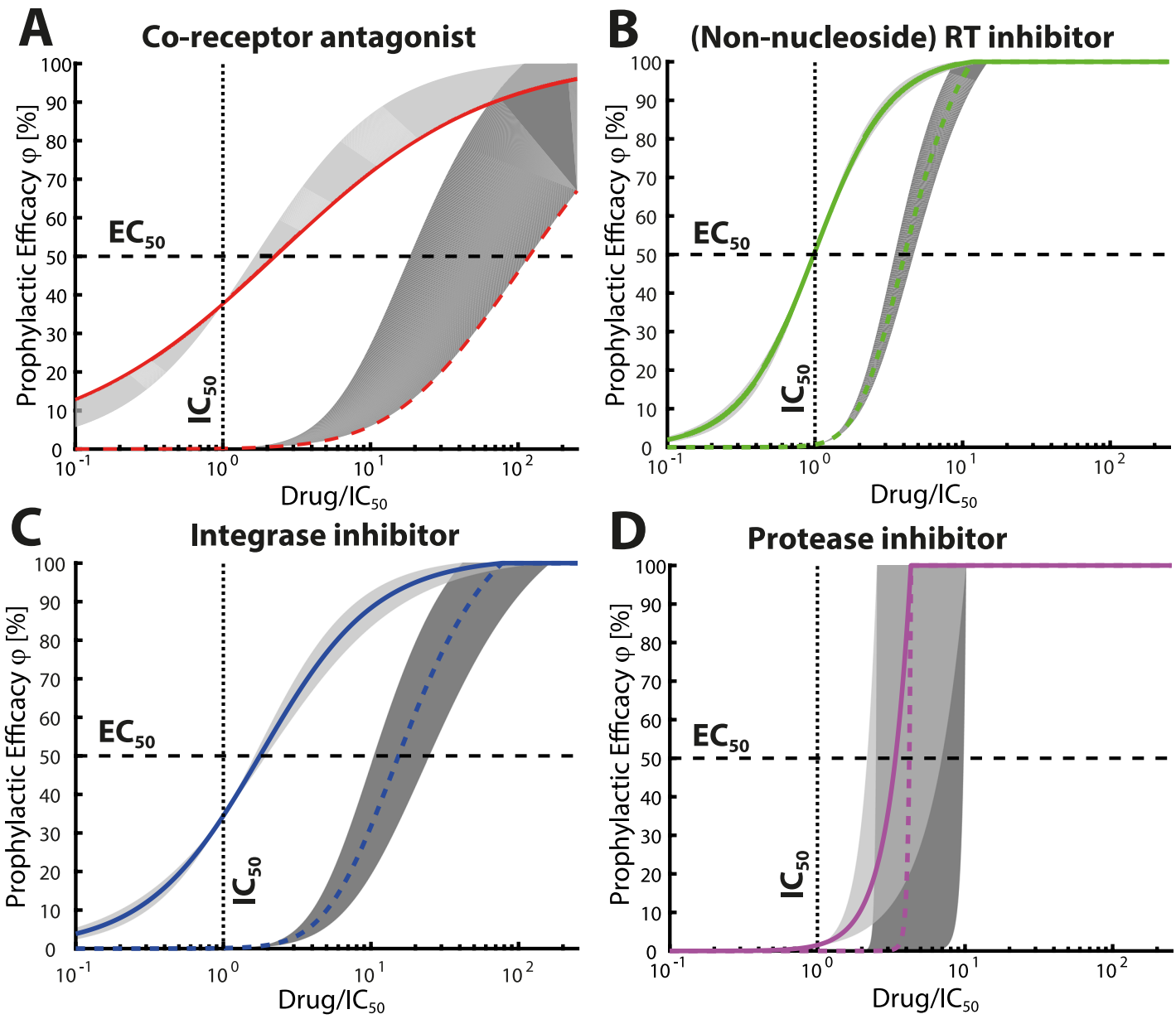

Fig 3. Shape of the concentration-prophylaxis profile. Colored lines depict the concentration-prophylaxis profile for an average drug class-specific slope parameter $\bar{m}$ in Eq (10). Solid colored line for an inoculum of one virus $Y_0 = \widehat{V}$ and dashed colored line for an inoculum of $Y_0 = 100 \cdot \widehat{V}$. Shaded areas indicate the concentration-prophylaxis profile for the smallest $m_{\min}$ and largest class-specific slope parameter $m_{\max}$ for the respective drug class as indicated in Table 2. **A**: Co-receptor antagonists. Currently only one co-receptor antagonist, maraviroc, is approved. We use $\bar{m} = m_{\min} = 0.61$ and also plot $m_{\max} = 1$ as a reference. **B**: Non-nucleoside reverse transcriptase inhibitors (NNRTIs); $\bar{m} = 1.71$, $m_{\min} = 1.55$ and $m_{\max} = 1.92$. Nucleoside reverse transcriptase inhibitors (NRTI) have been analyzed in [18]. **C**: Integrase inhibitors, $\bar{m} = 1.12$, $m_{\min} = 0.95$ and $m_{\max} = 1.3$. **D**: Protease inhibitors; $\bar{m} = 2.87$, $m_{\min} = 1.81$ and $m_{\max} = 4.53$. Utilized virus dynamics parameters are stated in Table 1.

https://doi.org/10.1371/journal.pcbi.1006740.g003

where $C << 1$ is a constant. Moreover, for realistic (large) $R_0(\varnothing) \gg 3$ their plasma concentration has to exceed their IC_{50} to decrease the probability of infection by at least 50%, Fig 3D. Similarly, we can rearrange the equation above and obtain

$$EC_x = IC_{50} \cdot \left(G \cdot \frac{x}{100}\right)^{1/m}, \tag{32}$$

for the exposure to a *to a single virus*, where $G := R_0(\varnothing) - 1$. Again, in case of exposure to multiple viruses, the slope parameter and EC_{50} increase, making the prophylactic efficacy of PIs exhibiting a switch-like behaviour as can be seen in Fig 3D. This switch-like behaviour makes the prophylactic use of PIs vulnerable to non-adherence, as well as general variations in concentrations (e.g. pharmacokinetics, inter-individual variability), and the prophylactic efficacy with these inhibitors may alternate between zero- or complete protection.

Prophylactic efficacy of treatment-approved antivirals

The combination of the nucleoside reverse transcriptase inhibitors (NRTIs) emtricitabine and tenofovir (Truvada) is the only intervention approved for pre-exposure prophylaxis (PrEP). According to our previous estimates [18], Truvada provides 96% protection in fully adherent individuals, which is in line with clinical estimates of 86-100% protection in the IPERGAY study [1], 58-96% in the PROUD study [2] and 96% in the Partners PrEP OLE study in apparently highly adherent individuals. The VOICE [3] and FEM-PrEP [52] studies indicated that Truvada may not prevent infection in poorly adherent individuals.

Currently, a number of drugs are under investigation for PrEP repurposing [6]. Notably, all currently investigated compounds are patent-protected and may not be affordable in resource-constrained countries hit hardest by the epidemic. In this work, we wanted to unselectively assess the utility of treatment-approved antivirals for prophylaxis and to assess whether currently neglected (patent-expired) compounds may be cost-efficient alternatives to be further explored in non-profit prophylaxis programmes.

We utilized comprehensive sets of drug-specific pharmacodynamic- and pharmacokinetic parameters (Table 2) to parameterize Eq (10) and to predict the prophylactic efficacy of treatment approved CRAs, non-nucleoside reverse transcriptase inhibitors (NNRTIs), InIs and PIs at clinically relevant concentration ranges (the class of NRTIs have been analyzed in earlier work [18]). Moreover, we sampled the extent of viral exposure (number of viruses transmitted and reaching a replication-enabling compartment; Eq (22)) from a previously parameterized distribution [18] that accurately reflects transmitter virus loads and drug-free infection probabilities after sexual contact. The resultant benchmark is depicted in Fig 4. Fig 4 allows for an initial screen of the utility of the various drugs for oral PrEP. Most analyzed drugs, except for maraviroc (MVC), raltegravir (RAL), elvitegravir (EVG) and nelfinavir (NFV), potently prevent infection at concentrations ranges typically encountered in fully adherent individuals during treatment (range between minimum- to maximum concentration, $[C_{min}; C_{max}]$). During prophylaxis, adherence to the dosing regimen is a major problem and we thus consider a lower bound concentration that would arise if the drug had not been taken for three days prior to exposure C_{low} (thin dashed vertical line in Fig 4) to emphasise a 'pharmacokinetic safety margin' in case of poor adherence. Numerical values for the computed maximum prophylactic efficacy and the efficacy at the lower bound concentrations are reported in Table 3 alongside with estimated EC_{50} and EC_{90} values. While in Table 3 we report the EC_{50} and EC_{90} values after challenge with a single virus $\widehat{V}$, the corresponding values after virus challenges sampled from the distribution for homosexual exposure Eq (24) were almost identical, see S4 Text for a comparison. Our simulations indicate a residual risk of infection for most analyzed drugs. Notably, most protease inhibitors may confer anything from none- to absolute protection within relevant concentration ranges, $[C_{low}; C_{max}]$, which highlights a severe limitation to their PrEP use in the context of poor adherence or pharmacokinetic (intra-/inter individual) variability. An exception among this rule is darunavir (DRV), which is predicted to be almost fully protective for the entire concentration range.

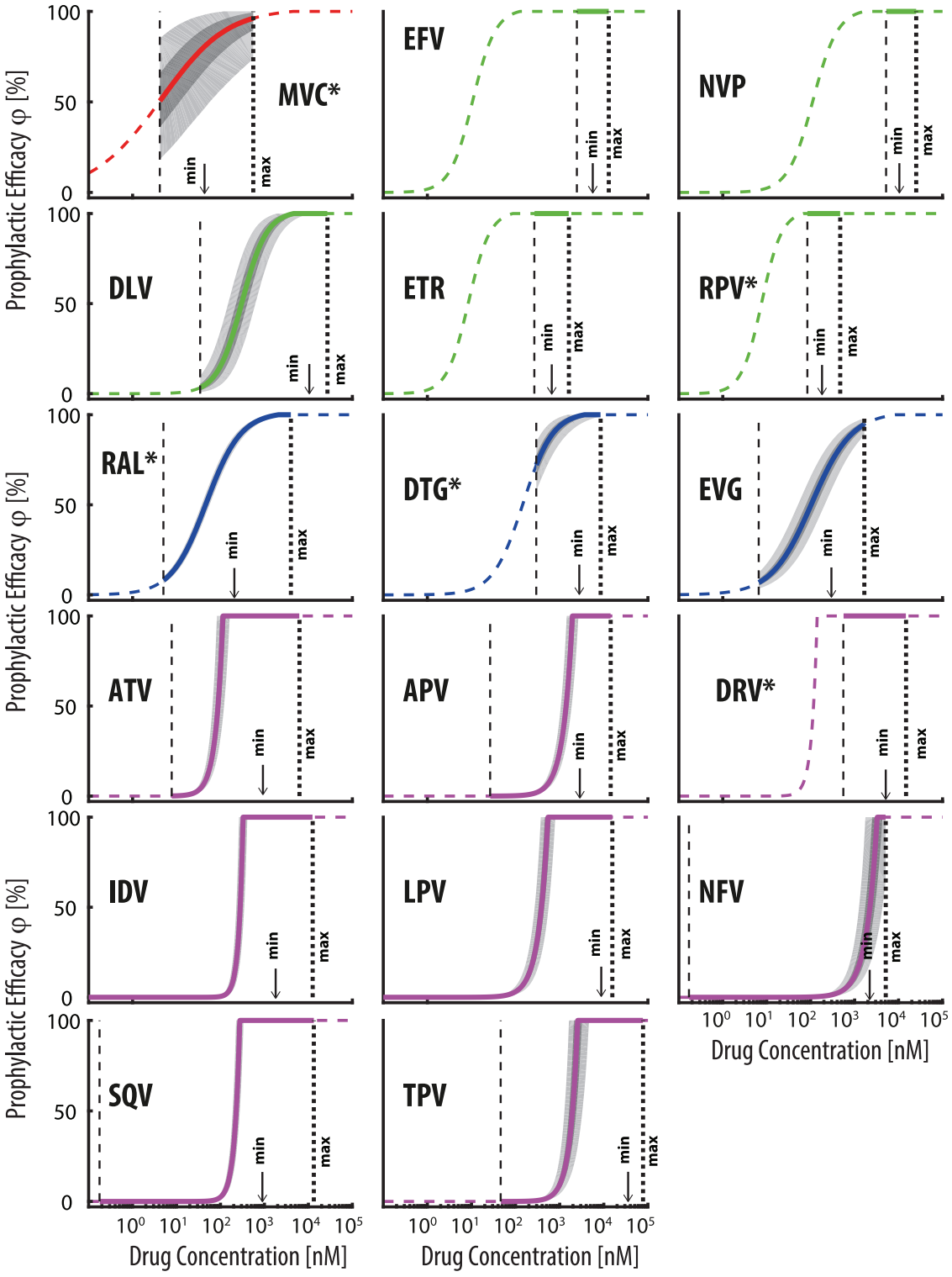

Fig 4. Drug specific prophylactic efficacy. Solid and dashed colored lines depict the concentration-prophylaxis profile for the individual drugs. The solid lines represent the concentration-prophylaxis profiles and light and dark grey areas indicate the quartile ranges and 5-95% ranges of the concentration-prophylaxis profile, considering uncertainty in pharmacodynamic parameters (Table 2) and the distribution of viral inoculum sizes after homosexual exposure to HIV using the virus exposure model' (Methods section and [18]). Maximum clinically achievable concentrations C_{max} for chronic oral administration of the standard dosing regimen and a lower bound concentration C_{low} that would be achieved if the last dose had been taken three days prior to virus

exposure are marked by thick and thin vertical black dashed lines respectively. For IDV, LPV, NFV and SQV C_{low} falls below the range of the x-axis. Downward pointing arrows indicate minimum (pre-dose) concentrations achieved for standard regimen in *adherent* individuals as reported in [40], [96] and [95]. MVC -maraviroc, EFV -efavirenz, NVP -nevirapine, DLV -delavirdine, ETR -etravirine, RPV -rilpivirine, RAL -raltegravir, EVG -elvitegravir, DTG -dolutegravir, ATV -atazanavir, APV -amprenavir, DRV -darunavir, IDV -indinavir, LPV -lopinavir, NFV -nelfinavir, SQV -saquinavir, TPV -tipranavir. *recently or currently tested for PrEP.

https://doi.org/10.1371/journal.pcbi.1006740.g004

Of the analyzed non-PI drugs, the NNRTIs efavirenz (EFV), nevirapine (NVP), etravirine (ETR) and rilpivirine (RPV) are extremely potent with regard to prophylaxis: These drugs prevent infection, even when the drug had not been taken for three consecutive days, Table 3. Notably, NVP and EFV are patent-expired and may represent suitable candidates for use in resource-constrained settings (price per day ≈ 0.1US$). The co-receptor antagonist maraviroc (MVC) and the integrase inhibitor dolutegravir (DTG) retain some prophylactic efficacy (50 and 72% respectively) at lower bound concentrations C_{low}. The CRA maraviroc (MVC), the NNRTI rilpivirine (RPV) and the InI raltegravir (RAL) are currently investigated for use as PrEP compounds (long-acting injections of RPV and RAL; oral- or topical application of MVC). In our simulations the predicted PrEP efficacy of these drugs would drop to 8% (RAL) and 50% (MVC) when the drug had not been taken for three consecutive days prior to virus exposure. Notably, RPV remained 100% effective.

Lastly, we want to note that our predictions are based on viral dynamics parameters that may under-predict prophylactic efficacy, as indicated in S2 Text. The main purpose of this modelling study was to rule out drug candidates, based on lack-off- or uncertain- prophylactic

Table 3. Prophylactic efficacy and sensitivity to incomplete adherence. The table shows the prophylactic efficacy (% reduction in infection probability) of all investigated drugs at their respective maximum achievable drug concentrations after chronic oral administration of the standard regimen and its efficacy at a concentration level that would be reached if the last dose had been taken least three days prior to virus exposure $C_{low} = C_{min} \cdot e^{-2.24 \cdot k_e}$, with $k_e = \ln(2)/t_{1/2}$ and halflifes $t_{1/2}$ reported in Table 2. The 5-95% range of these estimates are shown in brackets and consider uncertainty in pharmacodynamic parameters IC_{50}, m and variability in virus exposure after homosexual contact, according to the 'virus exposure model' (Methods section and Duwal et al. [18]. The last two columns show the EC_{50} and EC_{90} in the case when an individual was exposed to a single virus $\widehat{V}$. MVC -maraviroc, EFV -efavirenz, NVP -nevirapine, DLV -delavirdine, ETR -etravirine, RPV -rilpivirine, RAL -raltegravir, EVG -elvitegravir, DTG -dolutegravir, ATV -atazanavir, APV -amprenavir, DRV -darunavir, IDV -indinavir, LPV -lopinavir, NFV -nelfinavir, SQV -saquinavir, TPV -tipranavir. *currently investigated for PrEP.

	prophylactic efficacy φ [%]				$EC_{50}(\widehat{V})$	$EC_{90}(\widehat{V})$
drug	$\varphi(C_{max})$		$\varphi(C_{low})$		**[nM]**	**[nM]**
MVC*	96.10	(74.11;100)	50.12	(18.63;85.42)	11.45	349.63
EFV	100	(100;100)	100	(100;100)	10.55	36.23
NVP	100	(100;100)	100	(100;100)	114.06	438.06
DLV	100	(100;100)	3.38	(0.88;10.19)	329.50	1254.58
ETR	100	(100;100)	100	(100;100)	8.45	26.75
RPV*	100	(100;100)	100	(99.02;100)	7.61	22.55
RAL*	100	(100;100)	8.15	(6.32;10.23)	45.40	302.36
DTG*	100	(99.03;100)	72.12	(57.77;84.85)	145.18	722.23
EVG	94.61	(89.02;97.97)	6.96	(3.66;12.49)	108.66	976.25
ATV	100	(100;100)	0.08	(0.04;0.15)	87.44	108.79
APV	100	(100;100)	0.01	(0.01;0.03)	1394.96	1848
DRV*	100	(100;100)	100	(100;100)	118.32	139.24
IDV	100	(100;100)	0	(0;0)	280.80	319.71
LPV	100	(100;100)	0	(0;0)	389.69	519.09
NFV	100	(64.01;100)	0	(0;0)	2253.66	3118.34
SQV	100	(100;100)	0	(0;0)	227.29	266.66
TPV	100	(100;100)	0	(0;0.02)	1944.89	2458.09

https://doi.org/10.1371/journal.pcbi.1006740.t003

efficacy. While some drugs' prophylactic efficacy might be under-predicted, this *conservative* choice of parameters provides a more solid scientific basis for the remaining candidates that are predicted to be potent.

Discussion

Our intent was to develop a tool to screen out unsuitable candidates for PrEP based on unfavourable pharmacokinetic and pharmacodynamic characteristics. Clearly, the attributes which make any compound favourable extend beyond PK/PD, and critically also depend on tolerability, ease of dosing, cost and acceptability. Nevertheless, screening antiretroviral agents based on their intrinsic antiviral activity, mode of action, duration of efficacy beyond the dosing interval, and tolerance for missed dosing is a logical starting point when assessing potential candidates for PrEP.

Strikingly, we observed that *in vitro* measured drug potency may over-estimate PrEP potency in a drug-class specific manner. For all non-RTI drugs dosing schedules in clinical trials may have to be adjusted accordingly to reach the desired prophylaxis endpoints (% protection). We provide an easy-to-use software tool to determine the corresponding target concentrations (www.systems-pharmacology.org/prep-predictor).

For non-PI drugs, we observed a more graded relationship between their prophylactic efficacy and drug concentrations. At low virus inoculum sizes, the slope of their concentration-prophylaxis profile is largely determined by the slope coefficient that describes their direct effects [40]. Notably, for PIs we observed a very steep concentration prophylaxis profile, suggesting that within clinically relevant ranges for oral PrEP (Fig 4) their efficacy is likely to switch between zero- and complete protection, in an 'either-or' scenario. This characteristic renders PIs particularly vulnerable to poor adherence and drug-drug interactions. An intuitive explanation for this steep concentration-prophylaxis profile of PIs (power function in Eq (31)) is based on its unfortunate drug-to-target stoichiometry: A single late infected cell T_2 produces hundreds of infectious viruses on average (using parameters from Table 1 $a_6/a_3 = 670$) and a PI needs to prevent all of them from becoming infectious to fully prevent infection. By contrast, all other compounds only need to prevent a single viral entity from progressing, explaining the proportionality to the EMAX equation seen in Eqs (25)–(27).

By screening all treatment-approved antivirals for their PrEP utility, we predicted that efavirenz (EFV), nevirapine (NVP), etravirine (ETR), rilpivirine (RPV) and darunavir (DRV) may fully prevent infection after oral application and in case of poor adherence (Table 3 and Fig 4). Notably, these compounds have favourable inhibitory quotients (clinically achieved concentrations vastly exceed their EC_{50}) and their long elimination half-lives guarantees that inhibitory quotients stay in that favourable range. The drugs maraviroc (MVC) and dolutegravir (DTG) potently prevent infection but may allow for HIV transmission when individuals poorly adhere to the medication. Notably, the NNRTIs EFV, NVP, RPV and ETR exhibit long elimination half-lives (30-40h) and achieve concentrations required for PrEP to act quickly, and durably. However, there are some safety concerns with liver toxicity, which contraindicate e.g. the use of NVP in uninfected individuals. Liver toxicity to ETR remains to be elucidated in the context of prophylaxis. Skin reactions (ETR and EFV) and neuropsychiatric effects (EFV) have been reported in the context of HIV treatment that need to be evaluated in the context of potential PrEP applications. Likewise, skin reactions and rare liver toxicities with DRV need careful assessment in the context of PrEP repurposing. Moreover, the particular concentration-prophylaxis profile, as depicted in Fig 4, argues for a form of DRV administration that is not dependent on daily dosing for maintaining drug levels (e.g. slow release or nanoparticle formulations). For rilpivirine (RPV), our simulations suggest that near complete protection

can be achieved when concentrations exceed EC_{90}, Fig 4. RPV is currently investigated as a long-acting formulation in HPTN076 using 1200mg injections every 2 month which yields tough concentrations (median 186 nM) well in excess of this target. However, significant variability is still observed related to gender, and between injections on different occasions [51] which could be incorporated into future model generations. Besides rilpivirine, maraviroc (MVC; 300mg once daily), and raltegravir (RAL) are currently clinically investigated for oral PrEP. Our simulations suggest MVC may incompletely prevent infection even at maximum concentrations and that its efficacy steadily drops with declining levels down to 50% when the drug had not been taken for three days prior to exposure. Results from the NEXT-PrEP (HPTN 069) phase II study observed that MVC may not be potent enough on its own and that among those acquiring HIV infection, MVC concentrations were low, absent or variable [53]. Our model prediction is consistent with the reported lack of efficacy of MVC as PrEP in animals and human explant samples [54] and suggests that the potency of MVC, against infection may be less than its potency in preventing HIV replication ($EC_{50} > IC_{50}$, $EC_{90} > IC_{90}$). However, EC_{50}, EC_{90} estimates for co-receptor antagonists are highly parameter sensitive (S2 Text) warranting further research into elucidating the early infection dynamics. Using the parameters presented in Table 1, we estimate that the EC_{90} may be around 350nM, which is approximately 70 times larger than its IC_{50} (conversion formula provided in the results section). Notably, during the dose finding for MVC an IC_{90} of only 3.9nM (2ng/ml) was considered and this estimate was taken directly to determine target concentrations providing 90% prophylactic efficacy. Other compounds currently under investigation (HPTN-083) [55], but not evaluated in our study are the novel long-acting integrase inhibitor cabotegravir.

Our model has several limitations, but also a number of important advantages. Our simulations do not take into account drug concentrations at the site of mucosal exposure (e.g. cervix, rectum) [51, 56]. These concentrations have, however, not been validated as targets for successful prevention or treatment, whereas data exist (albeit limited) for plasma drug concentrations. Instead, we modelled based on *unbound* concentrations, in line with the broadly accepted 'free drug hypothesis'. Under the 'free drug hypothesis', the unbound concentrations are assumed to be available at the target site to exert pharmacological effects. For drugs highly bound to plasma protein (> 90%), naturally, their *total* concentrations at sites other than the plasma are magnitudes lower [56]. Strikingly, however, the unbound concentrations are identical [57]. Therefore, throughout the work, we assumed, according to the 'free drug hypothesis' [58] that the unbound concentrations in plasma and at the target site coincide, where the latter exerts the antiviral effect [59, 60]. All analyzed NNRTIs, InIs and PIs, except for raltegravir (RAL), are highly lipophilic, enabling the *unbound* drug to rapidly cross cellular membranes, generating an equilibrium between the *unbound* drug on either side of the cellular membrane [61]. Even for the weakly lipophilic compound raltegravir, intracellular concentrations are proportional to plasma concentrations by a factor precisely resembling their unbound moiety [62, 63], strongly arguing for the validity of the 'free drug hypothesis' for all analyzed drugs. However, ultimate proof in terms of local measurements in humans are lacking currently and may be difficult to obtain experimentally. On the contrary, nucleoside reverse transcriptase inhibitors (NRTIs), which we analysed in a previous work [18] are not expected to obey the 'free drug hypothesis' [17, 30, 64]. These compounds need to be actively taken up by cells and converted intracellularly into pharmacologically active triphosphates (NRTI-TP). Since the expression of transporters and intracellular enzymes is likely cell-specific, different cell types may contain vastly different concentrations of pharmacologically active compound. It is therefore entirely unclear what relevance concentration measurements of NRTI-TPs in tissue homogenates [65] (containing HIV target- and non-target cells) from sites of viral exposure (e.g. cervix, rectum) have in terms of prophylaxis.

Utilising the virus exposure model Eqs (23) and (24), we estimated the probability of virus clearance (and the prophylactic efficacy φ) as a function of the number of viruses ultimately reaching a target cell environment, and not as a function of mucosal exposure. The quantitative role of a number of physiological processes underlying primary infection is currently not fully resolved and impossible to measure in humans (e.g. the cells involved at the local site of exposure, their abundance, locations, their capabilities to transduce virus through physiological barriers and the respective R_0s). It is known however, that the virus has to overcome a number of physiological bottlenecks/barriers to reach a compartment that permits viral expansion. Despite the mucosal barrier, the sub-mucosal target cell density might initially be low [66], such that only a tiny fraction of viruses find a target cell before being cleared. It has also been reported [66–68], that target cells are subsequently recruited to the site of initial exposure due to inflammation and seminal exposure, mitigating the 'low target cell bottleneck' subsequently. If the low target-cell bottleneck is only prevalent during the first replication cycle it can also be modelled by simply considering a smaller virus inoculum that reaches a target-cell environment. In our approach, to obviate model- and parameter uncertainties, we chose a minimal/parsimoneous, data-driven approach that treats all physiological barriers as a single bottleneck lumped in terms of the 'success probability' r in Eq (24).

The target cell environment herein is a compartment that is decisive for establishing- and shedding infection (this compartment requires $R_0 > 1$). We also assumed that this compartment is well-perfused at the time scale of interest. Under this assumption, viral kinetic parameters measured in plasma coincide with kinetic parameters at the target cell environment, after converting the deterministic reaction parameters to their respective stochastic counterparts (Table 1).

Notably, the model (see Methods section) is calibrated [18] to reflect the per-contact infection risks for typical transmitter virus loads and different modes of sexual exposure (homo- and heterosexual), but can also be adapted to model intravenous exposure by e.g. injection. The calibrated virus exposure model [18] (see Methods section) predicts that either none- or a single infectious virus enter a replication enabling compartment in the majority of hetero-/homosexual contacts. Thus, we suggest that $EC_{50}(\widehat{V})$, $EC_{90}(\widehat{V})$ values stated in Table 3 provide a good proxy for the drug-specific prophylactic potency after sexual exposure to HIV (see also S4 Text for a comparison). Importantly, we also observed that increasing the inoculum size decreases the prophylactic efficacy of all drug classes considered (as suggested by increasing EC_{50} and EC_{90}) and increases the steepness of the concentration prophylaxis profile, Fig 3. PIs in particular displayed an almost switch-like prophylactic profile in the case of large inoculum sizes. These observations strikingly indicate that preventive target concentrations can depend on the route of transmission. I.e., intravenous exposure to HIV (larger inoculum sizes compared to sexual exposure) may require higher concentrations for HIV prevention.

When $R_0(\varnothing)$ is relatively large, we find that our predictions of prophylactic efficacy and -potency for or CRAs, RTIs and InIs are relatively invariant to parameter changes (compare Eqs (25)–(30)). However, we find that when considering an extremely broad range of $1.7 < R_0(\varnothing) < 112$ values, as in S2 Text, that the parameters used are rather *conservative* in the sense that they disfavour the drugs and may under-predict prophylactic efficacy. With regard to our work's aim (screen out candidates based on lack-off-, or uncertain potency) such a *conservative* parameter choice should be preferred. For PIs, although highly sensitive to changes R_0 (compare Eqs (31) and (32)) the qualitative statements made (the prophylactic potency is less than suggested by IC50, as well as the steep shape of the concentration-prophylaxis profile) are unaffected for arbitrary, yet realistic parameters, as analysed in S2 Text. However, in the provided software tool (www.systems-pharmacology.org/prep-predictor) it is possible to freely

change all virus dynamics parameters. Notably, Ribero et al. [69] have recently estimated $R_0 \approx 8$ during *acute* infection ($\leq$ 10 days after exposure, virus is detectable), which is much lower than the value used by us $R_0 \approx 67$, which considers viral replication immediately after exposure, in the so-called *eclipse phase* before virus becomes detectable. Our R_0 value is relatively high because we assume a lower CL (clearance of free virus) during this early phase of infection, in line with other modelling approaches [14, 33] and in line with the observation that adaptive immune responses develop only after about 14 days post exposure [70]. However, if we utilise CL = 23 (1/day), as in Ribero et al. [69], we obtain similar values of R_0.

The knowledge of concentration-prophylaxis relationships between drug classes, and for each component of a particular drug class allows for the intelligent design of PrEP regimens, including how quickly protection can be achieved after a loading dose and how forgiving the regimen is towards missed dosing events. In related article [27] we develop a sophisticated simulation framework that allows to make use of population pharmacokinetic models, to fully explore inter-individual pharmacokinetics and to assess sensitivity towards dosing, individual pharmacokinetic variability and timing of viral challenges.

Our model can be adapted or developed in a number of ways. On a technical side, the analytical solutions provided in the article can be neatly integrated into hybrid stochastic-deterministic algorithms that consider time-varying drug concentrations (pharmacokinetics), as outlined in an accompanying article [27]. In brief, therein we utilize analytic solutions for the extinction probability, Eq (22), to define a set of states where extinction is feasible (*extinction simplex*). Whenever trajectories leave the *extinction simplex*, simulations can be stopped and a hybrid stochastic-deterministic trajectory can be safely classified as an *infection event*. Regarding applications, the separate impact of treatment as prevention [71] (in the case of the donor) versus prophylactic efficacy in the exposed individual can be readily simulated by calibrating the virus load distribution in potential transmitter populations (see 'exposure model' in the Methods section). The effect of PrEP on the transmission of resistance can be estimated by altering $R_0(\varnothing)$ (the fitness cost of resistance) and by simultaneously increasing IC_{50} in Eq (10) (extent of resistance). The fitness cost of resistance translates into a decreased transmissibility of resistance in the absence of drugs (Eqs (19)–(21)), while the extent of resistance translates into an increased transmissibility relative to the wildtype at increasing drug concentrations, as e.g. illustrated in [18] (Figure 3 therein). Consequently, provided any transmitted resistance confers some fitness defect, prophylaxis may increase the frequency of transmitted resistance relative to the wildtype, but not its absolute occurrence [18, 72]. Since resistance to HIV drugs generally develops in a stepwise manner, the change in EC_{50} following acquisition of a resistance mutation can be introduced into this model, to identify a zone of selective pressure for the *de novo* evolution or spread of resistance under PrEP. However, during the early events when the virus infection can still be averted, the population size is too small for resistance to appear *de novo*: A single point mutation appears with probability $1 - (1 - \mu)^k$ at a particular base, where $\mu \approx 2.2 \cdot 10^{-5}$ is the per base mutation rate of HIV during reverse transcription [73] and k is the number of reverse transcription (= cell infection) events. Thus, *de novo* resistance can be assumed to appear, if e.g. PrEP had not been taken at the time of exposure, such that the infection expanded exponentially, and when PrEP is (re-)initiated some time after this early infection has been established. *De novo* resistance development in the context of poor adherence can be modelled in analogy to the work conducted by Rosenbloom et al. [74].

It is well known that the establishment of a latent reservoir is the major barrier to viral extinction during treatment [75] and this reservoir may be established as early as 3 days post infection [76, 77]. In the current framework, we computed viral extinction when $t \to \infty$, assuming drug concentrations stayed constant. Thus, extinction estimates are not affected by the inclusion of a long lived cellular compartment. In an accompanying article [27] we

overcome this assumption, explicitly considering drug pharmacokinetics and e.g. short-course prophylaxis. In the accompanying article infection of long lived cells are considered as an algorithmic stopping criterium: I.e., whenever long lived cells become infected, viral extinction is considered infeasible.

In summary, we have developed a mechanistic modelling tool to *a priori* screen antivirals for their prophylactic utility. Our approach revealed that *in vitro* measured drug potency (IC_{50}, IC_{90}) should not be used directly to identify lower bound effective concentrations in PrEP trials: With the exception of reverse transcriptase inhibitors, PrEP potency may be less than *in vitro* drug potency, i.e. higher concentrations of drug are required for prophylaxis than suggested by their *in vitro* potency. Consequently, when clinical trial design is guided by *in vitro* drug potency, prophylactic dosing regimen may be selected that attain insufficient concentrations to adequately prevent HIV infection.

Instead, we recommend to use the tool provided (www.systems-pharmacology.org/prep-predictor) to translate *in vitro* drug potency into prophylactic efficacy. We used the developed methods to assess the prophylactic utility of all treatment approved antivirals, allowing to rule out particular candidates by lack-of-, or uncertain prophylactic efficacy. To this end, we presented results using viral dynamics parameters that may under-predict prophylactic efficacy (S2 Text). These preliminary screens indicated that darunavir (DRV), efavirenz (EFV), nevirapine (NVP), etravirine (ETR) and rilpivirine (RPV) may fully prevent infection at concentrations typically achieved during treatment and with an adequate 'pharmacokinetic margin'. Notably, this prediction is robust across a wide range of (uncertain) parameters (S2 Text). Moreover, we predicted that maraviroc (MVC) and dolutegravir (DTG) can potently prevent infection, but that these drugs do not provide a comparable 'pharmacokinetic margin'. Furthermore, predictions for MVC are uncertain with respect to viral dynamics parameters (efficacy may both be over- or underpredicted). A next logical step is to further trim this candidate set by ruling out compounds with ominous safety profiles, followed by an assessment of different dosing (roll-out) schemes.

Supporting information

S1 Text. The Supplementary Text contains a step-by-step derivation of the equations for the extinction/infection probability presented in the main article.
(PDF)

S2 Text. The Supplementary Text contains a sensitivity analysis with respect to viral dynamics parameters.
(PDF)

S3 Text. The Supplementary Text contains details of the IC_{50}-to-EC_{50} conversion.
(PDF)

S4 Text. The Supplementary Text compares the EC_{50} and EC_{90} (antiviral concentrations that provide 50- and 90% protection) after viral challenge with (i) a single virus $\widehat{V}$, and after virus challenges (ii) sampled from the distribution for homosexual exposure, Eq (24).
(PDF)

S5 Text. The Supplementary Text contains details of the protein-binding adjustment for pharmacodynamic parameters.
(PDF)

Author Contributions

Conceptualization: Sulav Duwal, Max von Kleist.

Formal analysis: Sulav Duwal, Laura Dickinson, Saye Khoo, Max von Kleist.

Investigation: Sulav Duwal, Laura Dickinson, Max von Kleist.

Methodology: Sulav Duwal, Max von Kleist.

Project administration: Saye Khoo, Max von Kleist.

Software: Sulav Duwal.

Supervision: Saye Khoo, Max von Kleist.

Writing – original draft: Sulav Duwal, Max von Kleist.

Writing – review & editing: Laura Dickinson, Saye Khoo.

References

1. Grant R, Anderson P, McMahan V, Liu A, Amico K, Mehrotra M, et al. Results of the iPrEx open-label extension (iPrEx OLE) in men and transgender women who have sex with men: PrEP uptake, sexual practices, and HIV incidence. AIDS. 2014; p. 20–25.
2. McCormack S, Dunn DT, Desai M, Dolling DI, Gafos M, Gilson R, et al. Pre-exposure prophylaxis to prevent the acquisition of HIV-1 infection (PROUD): effectiveness results from the pilot phase of a pragmatic open-label randomised trial. Lancet. 2016; 387(10013):53–60. https://doi.org/10.1016/S0140-6736(15)00056-2 PMID: 26364263
3. Tenofovir-based preexposure prophylaxis for HIV infection among African women. N Engl J Med. 2015; 372:509–518. https://doi.org/10.1056/NEJMoa1402269 PMID: 25651245
4. Keller SB, Smith DM. The price of tenofovir-emtricitabine undermines the cost-effectiveness and advancement of pre-exposure prophylaxis. AIDS. 2011; 25(18):2308–2310. https://doi.org/10.1097/QAD.0b013e32834d3cab PMID: 22067201
5. Boffito M, Jackson A, Asboe D. Pharmacology lessons from chemoprophylaxis studies. Clin Infect Dis. 2014; 59 Suppl 1:S52–S54. https://doi.org/10.1093/cid/ciu250 PMID: 24926035
6. AIDS Vaccine Advocacy Coalition. Pre-Exposure Prophylaxis (PrEP) by the Numbers, (available at http://www.avac.org/sites/default/files/resource-files/prep_BTN_aug2016.pdf, accessed 22-Oct-2017.).
7. Gomez GB, Borquez A, Case KK, Wheelock A, Vassall A, Hankins C. The cost and impact of scaling up pre-exposure prophylaxis for HIV prevention: a systematic review of cost-effectiveness modelling studies. PLoS Med. 2013; 10:e1001401. https://doi.org/10.1371/journal.pmed.1001401 PMID: 23554579
8. Abbas UL, Glaubius R, Mubayi A, Hood G, Mellors JW. Antiretroviral therapy and pre-exposure prophylaxis: combined impact on HIV transmission and drug resistance in South Africa. J Infect Dis. 2013; 208:224–234. https://doi.org/10.1093/infdis/jit150 PMID: 23570850
9. Supervie V, Barrett M, Kahn JS, Musuka G, Moeti TL, Busang L, et al. Modeling dynamic interactions between pre-exposure prophylaxis interventions & treatment programs: predicting HIV transmission & resistance. Sci Rep. 2011; 1:185. https://doi.org/10.1038/srep00185 PMID: 22355700
10. Supervie V, Garcia-Lerma JG, Heneine W, Blower S. HIV, transmitted drug resistance, and the paradox of preexposure prophylaxis. PNAS. 2010; 107:12381–12386. https://doi.org/10.1073/pnas.1006061107 PMID: 20616092
11. Dimitrov D, Boily MC, Brown ER, Hallett TB. Analytic review of modeling studies of ARV Based PrEP interventions reveals strong influence of drug-resistance assumptions on the population-level effectiveness. PloS one. 2013; 8:e80927. https://doi.org/10.1371/journal.pone.0080927 PMID: 24282559
12. Hendrix CW. Exploring concentration response in HIV pre-exposure prophylaxis to optimize clinical care and trial design. Cell. 2013; 155(3):515–518. https://doi.org/10.1016/j.cell.2013.09.030 PMID: 24243011
13. Conway JM, Konrad BP, Coombs D. Stochastic analysis of pre- and postexposure prophylaxis against HIV infection. SIAM J Appl Math. 2013; 73(2):904–28. https://doi.org/10.1137/120876800
14. Tuckwell HC, Shipman PD, Perelson AS. The probability of HIV infection in a new host and its reduction with microbicides. Math Biosci. 2008; 214(1-2):81–86. https://doi.org/10.1016/j.mbs.2008.03.005 PMID: 18445499

15. Pearson JE, Krapivsky P, Perelson AS. Stochastic theory of early viral infection: continuous versus burst production of virions. PLoS Comput Biol. 2011; 7(2):e1001058. https://doi.org/10.1371/journal.pcbi.1001058 PMID: 21304934

16. Yan AWC, Cao P, McCaw JM. On the extinction probability in models of within-host infection: the role of latency and immunity. J Math Biol. 2016; 73:787–813. https://doi.org/10.1007/s00285-015-0961-5 PMID: 26748917

17. Duwal S, Schütte C, von Kleist M. Pharmacokinetics and pharmacodynamics of the reverse transcriptase inhibitor tenofovir and prophylactic efficacy against HIV-1 infection. PLoS One. 2012; 7(7):e40382. https://doi.org/10.1371/journal.pone.0040382 PMID: 22808148

18. Duwal S, Sunkara V, von Kleist M. Multiscale Systems-Pharmacology Pipeline to Assess the Prophylactic Efficacy of NRTIs Against HIV-1. CPT Pharmacometrics Syst Pharmacol. 2016; 5(7):377–387. https://doi.org/10.1002/psp4.12095 PMID: 27439573

19. Carlson JM, Schaefer M, Monaco DC, Batorsky R, Claiborne DT, Prince J, et al. HIV transmission. Selection bias at the heterosexual HIV-1 transmission bottleneck. Science. 2014; 345(6193):1254031. https://doi.org/10.1126/science.1254031 PMID: 25013080

20. Royce RA, Seña A, Cates W Jr, Cohen MS. Sexual transmission of HIV. N Engl J Med. 1997; 336 (15):1072–1078. https://doi.org/10.1056/NEJM199704103361507 PMID: 9091805

21. Boily MC, Baggaley RF, Wang L, Masse B, White RG, Hayes RJ, et al. Heterosexual risk of HIV-1 infection per sexual act: systematic review and meta-analysis of observational studies. Lancet Infect Dis. 2009; 9(2):118–129. https://doi.org/10.1016/S1473-3099(09)70021-0 PMID: 19179227

22. Keele BF, Giorgi EE, Salazar-Gonzalez JF, Decker JM, Pham KT, Salazar MG, et al. Identification and characterization of transmitted and early founder virus envelopes in primary HIV-1 infection. PNAS. 2008; 105(21):7552–7557. https://doi.org/10.1073/pnas.0802203105 PMID: 18490657

23. Abrahams MR, Anderson JA, Giorgi EE, Seoighe C, Mlisana K, Ping LH, et al. Quantitating the multiplicity of infection with human immunodeficiency virus type 1 subtype C reveals a non-poisson distribution of transmitted variants. J Virol. 2009; 83(8):3556–3567. https://doi.org/10.1128/JVI.02132-08 PMID: 19193811

24. Fischer W, Ganusov VV, Giorgi EE, Hraber PT, Keele BF, Leitner T, et al. Transmission of single HIV-1 genomes and dynamics of early immune escape revealed by ultra-deep sequencing. PloS one. 2010; 5 (8):e12303. https://doi.org/10.1371/journal.pone.0012303 PMID: 20808830

25. Li H, Bar KJ, Wang S, Decker JM, Chen Y, Sun C, et al. High Multiplicity Infection by HIV-1 in Men Who Have Sex with Men. PLoS Pathog. 2010; 6(5):e1000890. https://doi.org/10.1371/journal.ppat.1000890 PMID: 20485520

26. Allen LJS. An Introduction to Stochastic Processes with Applications to Biology. Chapman & Hall/CR; 2011.

27. Duwal S, Dickinson L, Khoo S, von Kleist M. Hybrid stochastic framework predicts efficacy of prophylaxis against HIV: An example with different dolutegravir prophylaxis schemes. PLoS Comput. Biol. 2018, 14(6):e1006155. https://doi.org/10.1371/journal.pcbi.1006155 PMID: 29902179

28. von Kleist M, Menz S, Huisinga W. Drug-class specific impact of antivirals on the reproductive capacity of HIV. PLoS Comput Biol. 2010; 6(3):e1000720. https://doi.org/10.1371/journal.pcbi.1000720 PMID: 20361047

29. von Kleist M, Menz S, Stocker H, Arasteh K, Schütte C, Huisinga W. HIV Quasispecies Dynamics during Pro-active Treatment Switching: Impact on Multi-Drug Resistance and Resistance Archiving in Latent Reservoirs. PLoS One. 2011; 6(3):e18204. https://doi.org/10.1371/journal.pone.0018204 PMID: 21455303

30. Duwal S, von Kleist M. Top-down and bottom-up modeling in system pharmacology to understand clinical efficacy: An example with NRTIs of HIV-1. Eur J Pharm Sci. 2016; 94:72–83. https://doi.org/10.1016/j.ejps.2016.01.016 PMID: 26796142

31. Isaacman-Beck J, Hermann EA, Yi Y, Ratcliffe SJ, Mulenga J, Allen S, et al. Heterosexual transmission of human immunodeficiency virus type 1 subtype C: Macrophage tropism, alternative coreceptor use, and the molecular anatomy of CCR5 utilization. J Virol. 2009; 83(16):8208–8220. https://doi.org/10.1128/JVI.00296-09 PMID: 19515785

32. Ping LH, Joseph SB, Anderson JA, Abrahams MR, Salazar-Gonzalez JF, Kincer LP, et al. Comparison of viral Env proteins from acute and chronic infections with subtype C human immunodeficiency virus type 1 identifies differences in glycosylation and CCR5 utilization and suggests a new strategy for immunogen design. J Virol. 2013; 87(13):7218–7233. https://doi.org/10.1128/JVI.03577-12 PMID: 23616655

33. Tan WY, Wu H. Stochastic modeling of the dynamics of CD4+ T-cell infection by HIV and some Monte Carlo studies. Math Biosci. 1998; 147(2):173–205. https://doi.org/10.1016/S0025-5564(97)00094-1 PMID: 9433062

34. Stafford MA, Corey L, Cao Y, Daar ES, Ho DD, Perelson AS. Modeling plasma virus concentration during primary HIV infection. J Theor Biol. 2000; 203(3):285–301. https://doi.org/10.1006/jtbi.2000.1076 PMID: 10716909

35. Perelson AS. Modelling viral and immune system dynamics. Nat Rev Immunol. 2002; 2(1):28–36. https://doi.org/10.1038/nri700 PMID: 11905835

36. Perelson AS, Kirschner DE, De Boer R. Dynamics of HIV infection of CD4+ T cells. Math Biosci. 1993; 114(1):81–125. https://doi.org/10.1016/0025-5564(93)90043-A PMID: 8096155

37. Pierson TC, Zhou Y, Kieffer TL, Ruff CT, Buck C, Siliciano RF. Molecular characterization of preintegration latency in human immunodeficiency virus type 1 infection. J Virol. 2002; 76(17):8518–8531. PMID: 12163571

38. Zhou Y, Zhang H, Siliciano JD, Siliciano RF. Kinetics of human immunodeficiency virus type 1 decay following entry into resting CD4+ T cells. J Virol. 2005; 79(4):2199–2210. https://doi.org/10.1128/JVI.79.4.2199-2210.2005 PMID: 15681422

39. Chou TC. Theoretical basis, experimental design, and computerized simulation of synergism and antagonism in drug combination studies. Pharmacolog Rev. 2006; 58(3):621–681. https://doi.org/10.1124/pr.58.3.10

40. Shen L, Peterson S, Sedaghat AR, McMahon MA, Callender M, Zhang H, et al. Dose-response curve slope sets class-specific limits on inhibitory potential of anti-HIV drugs. Nat Med. 2008; 14(7):762–766. https://doi.org/10.1038/nm1777 PMID: 18552857

41. Heffernan JM, Smith RJ, Wahl LM. Perspectives on the basic reproductive ratio. J R Soc Interface. 2005; 2:281–293. https://doi.org/10.1098/rsif.2005.0042 PMID: 16849186

42. Joseph SB, Swanstrom R, Kashuba ADM, Cohen MS. Bottlenecks in HIV-1 transmission: insights from the study of founder viruses. Nat Rev Microbiol. 2015; 13(7):414–25. https://doi.org/10.1038/nrmicro3471 PMID: 26052661

43. Powers KA, Poole C, Pettifor AE, Cohen MS. Rethinking the heterosexual infectivity of HIV-1: a systematic review and meta-analysis. Lancet Infect Dis. 2008; 8(9):553–563. https://doi.org/10.1016/S1473-3099(08)70156-7 PMID: 18684670

44. Quinn TC, Wawer MJ, Sewankambo N, Serwadda D, Li C, Wabwire-Mangen F, et al. Viral load and heterosexual transmission of human immunodeficiency virus type 1. Rakai Project Study Group. N Engl J Med. 2000; 342(13):921–929. https://doi.org/10.1056/NEJM200003303421303 PMID: 10738050

45. Mellors JW, Rinaldo C Jr, Gupta P, White RM, Todd JA, Kingsley LA. Prognosis in HIV-1 infection predicted by the quantity of virus in plasma. Science. 1996; 272(5265):1167–1170. https://doi.org/10.1126/science.272.5265.1167 PMID: 8638160

46. Yousef KP, Meixenberger K, Smith MR, Somogyi S, Gromöller S, Schmidt D, et al. Inferring HIV-1 Transmission Dynamics in Germany From Recently Transmitted Viruses. JAIDS Journal of Acquired Immune Deficiency Syndromes. 2016; 73(3):356–363. https://doi.org/10.1097/QAI.0000000000001122

47. Wilson DP, Law MG, Grulich AE, Cooper DA, Kaldor JM. Relation between HIV viral load and infectiousness: a model-based analysis. Lancet. 2008; 372(9635):314–320. https://doi.org/10.1016/S0140-6736(08)61115-0 PMID: 18657710

48. Attia S, Egger M, Müller M, Zwahlen M, Low N. Sexual transmission of HIV according to viral load and antiretroviral therapy: systematic review and meta-analysis. AIDS. 2009; 23(11):1397–1404. https://doi.org/10.1097/QAD.0b013e32832b7dca PMID: 19381076

49. Hughes JP, Baeten JM, Lingappa JR, Magaret AS, Wald A, de Bruyn G, et al. Determinants of per-coital-act HIV-1 infectivity among African HIV-1-serodiscordant couples. J Infect Dis. 2012; 205(3):358–365. https://doi.org/10.1093/infdis/jir747 PMID: 22241800

50. von Kleist M, Metzner P, Marquet R, Schütte C. HIV-1 polymerase inhibition by nucleoside analogs: cellular- and kinetic parameters of efficacy, susceptibility and resistance selection. PLoS Comput Biol. 2012; 8(1):e1002359. https://doi.org/10.1371/journal.pcbi.1002359 PMID: 22275860

51. McGowan I, Dezzutti CS, Siegel A, Engstrom J, Nikiforov A, Duffill K, et al. Long-acting rilpivirine as potential pre-exposure prophylaxis for HIV-1 prevention (the MWRI-01 study): an open-label, phase 1, compartmental, pharmacokinetic and pharmacodynamic assessment. Lancet HIV. 2016; 3:e569–e578. https://doi.org/10.1016/S2352-3018(16)30113-8 PMID: 27658864

52. Van Damme L, Corneli A, Ahmed K, Agot K, Lombaard J, Kapiga S, et al. Preexposure prophylaxis for HIV infection among African women. The New England journal of medicine. 2012; 367:411–422. https://doi.org/10.1056/NEJMoa1202614 PMID: 22784040

53. Gulick RM, Wilkin TJ, Chen YQ, Landovitz RJ, Amico KR, Young AM, et al. Phase 2 Study of the Safety and Tolerability of Maraviroc-Containing Regimens to Prevent HIV Infection in Men Who Have Sex With

Men (HPTN 069/ACTG A5305). Journal Infect Dis. 2017; 215:238–246. https://doi.org/10.1093/infdis/jiw525 PMID: 27811319

54. McGowan I, Nikiforov A, Young A, Cranston R, Landovitz RJ, Bakshi R, et al. PrEP Impact on T-Cell Activation and Explant Infection: HPTN 069/ACTG 5305 Substudy. In: CROI2016, Boston. Oral presentation 104; 2016.

55. Markowitz M, Frank I, Grant RM, Mayer KH, Elion R, Goldstein D, et al. Safety and tolerability of long-acting cabotegravir injections in HIV-uninfected men (ECLAIR): a multicentre, double-blind, randomised, placebo-controlled, phase 2a trial. Lancet HIV. 2017; 4:e331–e340. https://doi.org/10.1016/S2352-3018(17)30068-1 PMID: 28546090

56. Else LJ, Taylor S, Back DJ, Khoo SH. Pharmacokinetics of antiretroviral drugs in anatomical sanctuary sites: the male and female genital tract. Antivir Ther. 2011; 16:1149–1167. https://doi.org/10.3851/IMP1919 PMID: 22155899

57. Avery LB, Bakshi RP, Cao YJ, Hendrix CW. The male genital tract is not a pharmacological sanctuary from efavirenz. Clin Pharmacol Ther. 2011; 90:151–156. https://doi.org/10.1038/clpt.2011.99 PMID: 21633344

58. Smith DA, Di L, Kerns EH. The effect of plasma protein binding on in vivo efficacy: misconceptions in drug discovery. Nat Rev Drug Discov. 2010; 9(12):929–939. https://doi.org/10.1038/nrd3287 PMID: 21119731

59. Watkins WJ, Desai MC. HCV versus HIV drug discovery: Déjà vu all over again? Bioorg Med Chem Lett. 2013; 23(8):2281–2287. https://doi.org/10.1016/j.bmcl.2013.02.070 PMID: 23489621

60. Boffito M, Back DJ, Blaschke TF, Rowland M, Bertz RJ, Gerber JG, et al. Protein binding in antiretroviral therapies. AIDS Res Hum Retroviruses. 2003; 19(9):825–835. https://doi.org/10.1089/088922203769232629 PMID: 14585213

61. von Kleist M, Huisinga W. Physiologically based pharmacokinetic modelling: a sub-compartmentalized model of tissue distribution. J Pharmacokinet Pharmacodyn. 2007; 34:789–806. https://doi.org/10.1007/s10928-007-9071-3 PMID: 17899329

62. Sandkovsky U, Swindells S, Robbins BL, Nelson SR, Acosta EP, Fletcher CV. Measurement of plasma and intracellular concentrations of raltegravir in patients with HIV infection. AIDS. 2012; 26:2257–2259. https://doi.org/10.1097/QAD.0b013e328359a978 PMID: 22948265

63. Wang L, Soon GH, Seng KY, Li J, Lee E, Yong EL, et al. Pharmacokinetic modeling of plasma and intracellular concentrations of raltegravir in healthy volunteers. Antimicrob Agents Chemother. 2011; 55:4090–4095. https://doi.org/10.1128/AAC.00593-11 PMID: 21746959

64. von Kleist M, Huisinga W. Pharmacokinetic-pharmacodynamic relationship of NRTIs and its connection to viral escape: an example based on zidovudine. Eur J Pharm Sci. 2009; 36(4-5):532–543. https://doi.org/10.1016/j.ejps.2008.12.010 PMID: 19150497

65. Cottrell ML, Yang KH, Prince HMA, Sykes C, White N, Malone S, et al. A Translational Pharmacology Approach to Predicting HIV Pre-Exposure Prophylaxis Outcomes in Men and Women Using Tenofovir Disoproxil Fumarate +/- Emtricitabine. J Infect Dis. 2016.

66. Haase AT. Targeting early infection to prevent HIV-1 mucosal transmission. Nature. 2010; 464(7286):217–23. https://doi.org/10.1038/nature08757 PMID: 20220840

67. Li Q, Estes JD, Schlievert PM, Duan L, Brosnahan AJ, Southern PJ, et al. Glycerol monolaurate prevents mucosal SIV transmission. Nature. 2009; 458(7241):1034–8. https://doi.org/10.1038/nature07831 PMID: 19262509

68. Haaland RE, Hawkins PA, Salazar-Gonzalez J, Johnson A, Tichacek A, Karita E, et al. Inflammatory genital infections mitigate a severe genetic bottleneck in heterosexual transmission of subtype A and C HIV-1. PLoS Pathog. 2009; 5(1):e1000274. https://doi.org/10.1371/journal.ppat.1000274 PMID: 19165325

69. Ribeiro RM, Qin L, Chavez LL, Li D, Self SG, Perelson AS. Estimation of the initial viral growth rate and basic reproductive number during acute HIV-1 infection. J Virol. 2010; 84(12):6096–102. https://doi.org/10.1128/JVI.00127-10 PMID: 20357090

70. McMichael AJ, Borrow P, Tomaras GD, Goonetilleke N, Haynes BF. The immune response during acute HIV-1 infection: clues for vaccine development. Nat Rev Immunol. 2010; 10(1):11–23. https://doi.org/10.1038/nri2674 PMID: 20010788

71. Cohen MS, Chen YQ, McCauley M, Gamble T, Hosseinipour MC, Kumarasamy N, et al. Prevention of HIV-1 infection with early antiretroviral therapy. N Engl J Med. 2011; 365(6):493–505. https://doi.org/10.1056/NEJMoa1105243 PMID: 21767103

72. Frank M, von Kleist M, Kunz A, Harms G, Schütte C, Kloft C. Quantifying the impact of nevirapine-based prophylaxis strategies to prevent mother-to-child transmission of HIV-1: a combined pharmacokinetic, pharmacodynamic, and viral dynamic analysis to predict clinical outcomes. Antimicrob

Agents Chemother. 2011; 55(12):5529–5540. https://doi.org/10.1128/AAC.00741-11 PMID: 21947390

73. Mansky LM, Temin HM. Lower in vivo mutation rate of human immunodeficiency virus type 1 than that predicted from the fidelity of purified reverse transcriptase. J Virol. 1995; 69:5087–5094. PMID: 7541846

74. Rosenbloom DIS, Hill AL, Rabi SA, Siliciano RF, Nowak MA. Antiretroviral dynamics determines HIV evolution and predicts therapy outcome. Nat Med. 2012; 18:1378–1385. https://doi.org/10.1038/nm.2892 PMID: 22941277

75. Chun TW, Moir S, Fauci AS. HIV reservoirs as obstacles and opportunities for an HIV cure. Nat Immunol. 2015; 16(6):584–589. https://doi.org/10.1038/ni.3152 PMID: 25990814

76. Whitney JB, Hill AL, Sanisetty S, Penaloza-MacMaster P, Liu J, Shetty M, et al. Rapid seeding of the viral reservoir prior to SIV viraemia in rhesus monkeys. Nature. 2014; 512:74–77. https://doi.org/10.1038/nature13594 PMID: 25042999

77. Chun TW, Engel D, Berrey MM, Shea T, Corey L, Fauci AS. Early establishment of a pool of latently infected, resting CD4(+) T cells during primary HIV-1 infection. PNAS. 1998; 95:8869–8873. https://doi.org/10.1073/pnas.95.15.8869 PMID: 9671771

78. Wei X, Ghosh SK, Taylor ME, Johnson VA, Emini EA, Deutsch P, et al. Viral dynamics in human immunodeficiency virus type 1 infection. Nature. 1995; 373(6510):117–122. https://doi.org/10.1038/373117a0 PMID: 7529365

79. Sedaghat AR, Siliciano RF, Wilke CO. Constraints on the dominant mechanism for HIV viral dynamics in patients on raltegravir. Antivir Ther. 2009; 14(2):263–271. PMID: 19430101

80. Sedaghat AR, Dinoso JB, Shen L, Wilke CO, Siliciano RF. Decay dynamics of HIV-1 depend on the inhibited stages of the viral life cycle. PNAS. 2008; 105(12):4832–4837. https://doi.org/10.1073/pnas.0711372105 PMID: 18362342

81. Markowitz M, Louie M, Hurley A, Sun E, Mascio MD, Perelson AS, et al. A novel antiviral intervention results in more accurate assessment of human immunodeficiency virus type 1 replication dynamics and T-cell decay in vivo. J Virol. 2003; 77:5037–5038. https://doi.org/10.1128/JVI.77.8.5037-5038.2003 PMID: 12663814

82. Koelsch KK, Liu L, Haubrich R, May S, Havlir D, Günthard HF, et al. Dynamics of total, linear nonintegrated, and integrated HIV-1 DNA in vivo and in vitro. J Infect Dis. 2008; 197(3):411–419. https://doi.org/10.1086/525283 PMID: 18248304

83. Almond LM, Hoggard PG, Edirisinghe D, Khoo SH, Back DJ. Intracellular and plasma pharmacokinetics of efavirenz in HIV-infected individuals. J Antimicrob Chemother. 2005; 56(4):738–744. https://doi.org/10.1093/jac/dki308 PMID: 16141277

84. Cheng CL, Smith DE, Carver PL, Cox SR, Watkins PB, Blake DS, et al. Steady-state pharmacokinetics of delavirdine in HIV-positive patients: Effect on erythromycin breath test. Clin Pharmacol Ther. 1997; 61(5):531–543. https://doi.org/10.1016/S0009-9236(97)90133-8 PMID: 9164415

85. Brown KC, Patterson KB, Jennings SH, Malone SA, Shaheen NJ, Prince HMA, et al. Single and multiple dose pharmacokinetics of darunavir plus ritonavir and etravirine in semen and rectal tissue of HIV-negative men. J Acquir Immune Defic Syndr. 2012; 61(2):138. https://doi.org/10.1097/QAI.0b013e31825cb645 PMID: 22614898

86. Schöller-Gyüre M, Kakuda TN, Raoof A, De Smedt G, Hoetelmans RM. Clinical pharmacokinetics and pharmacodynamics of etravirine. Clinical pharmacokinetics. 2009; 48(9):561–574. https://doi.org/10.2165/10895940-000000000-00000 PMID: 19725591

87. Dickinson L, Bracchi M, Elliot E, Else L, Khoo S, Back D, et al. Population pharmacokinetics (PK) of dolutegravir (DTG) alone and following treatment switch. In: Journal of the International AIDS Society. vol. 19. INT AIDS SOCIETY AVENUE DE FRANCE 23, GENEVA, 1202, SWITZERLAND; 2016.

88. Delille CA, Pruett ST, Marconi VC, Lennox JL, Armstrong WS, Arrendale RF, et al. Effect of protein binding on unbound atazanavir and darunavir cerebrospinal fluid concentrations. J Clin Pharmacol. 2014; 54(9):1063–1071. https://doi.org/10.1002/jcph.298 PMID: 24691856

89. Letendre SL, Capparelli EV, Ellis RJ, McCutchan JA, Group HNRC, et al. Indinavir population pharmacokinetics in plasma and cerebrospinal fluid. Antimicrobial agents and chemotherapy. 2000; 44(8):2173–2175. https://doi.org/10.1128/AAC.44.8.2173-2175.2000 PMID: 10898694

90. Holladay JW, Dewey MJ, Michniak BB, Wiltshire H, Halberg DL, Weigl P, et al. Elevated alpha-1-acid glycoprotein reduces the volume of distribution and systemic clearance of saquinavir. Drug Metab Dispos. 2001; 29(3):299–303. PMID: 11181499

91. Veldkamp AI, van Heeswijk RP, Mulder JW, Meenhorst PL, Schreij G, van der Geest S, et al. Steady-state pharmacokinetics of twice-daily dosing of saquinavir plus ritonavir in HIV-1-infected individuals. JAIDS. 2001; 27(4):344–349. PMID: 11468422

92. Laskey SB, Siliciano RF. Quantitative evaluation of the antiretroviral efficacy of dolutegravir. JCI Insight. 2016; 1(19):e90033. https://doi.org/10.1172/jci.insight.90033 PMID: 27882352

93. Jilek BL, Zarr M, Sampah ME, Rabi SA, Bullen CK, Lai J, et al. A quantitative basis for antiretroviral therapy for HIV-1 infection. Nat Med. 2012; 18(3):446–451. https://doi.org/10.1038/nm.2649 PMID: 22344296

94. Dickinson L, Bracchi M, Elliot E, Else L, Khoo S, Back D, et al. Population pharmacokinetics (PK) of dolutegravir (DTG) alone and following treatment switch. In: International Congress of Drug Therapy in HIV Infection, Glasgow, UK. Abstract P094; 2016.

95. Crauwels HM, van Heeswijk RP, Vandevoorde A, Buelens A, Stevens M, Hoetelmans RM. The effect of rilpivirine on the pharmacokinetics of methadone in HIV-negative volunteers. J Clin Pharmacol. 2014; 54(2):133–140. https://doi.org/10.1002/jcph.222 PMID: 24203510

96. Kakuda TN, Abel S, Davis J, Hamlin J, Schöller-Gyüre M, Mack R, et al. Pharmacokinetic interactions of maraviroc with darunavir/ritonavir, maraviroc with etravirine, and maraviroc with etravirine/darunavir/ritonavir in healthy volunteers: results of two drug interaction trials. Antimicrob Agents Chemother. 2011; 55:2290–6. https://doi.org/10.1128/AAC.01046-10 PMID: 21383098